Earth and Space Science

RESEARCH ARTICLE
10.1029/2020EA001141

Intraregional Comparisons of the Near-Storm Environments of Storms Dominated by Frequent Positive Versus Negative Cloud-to-Ground Flashes

A. J. Eddy[1,2], D. R. MacGorman[1,2,3], C. R. Homeyer[2], and E. Williams[4]

[1]Cooperative Institute for Mesoscale Meteorological Studies, University of Oklahoma and NOAA/National Severe Storms Laboratory (NSSL), Norman, OK, USA, [2]School of Meteorology, University of Oklahoma, Norman, OK, USA, [3]NSSL, Norman, OK, USA, [4]Massachusetts Institute of Technology, Cambridge, MA, USA

Key Points:

- Storms dominated by frequent positive or negative ground flashes were mined from 11 years of National Lightning Detection Network data
- The near-storm environments of storms dominated by frequent positive or negative ground flashes were compared in each of seven regions
- The combination of environmental parameters inferred to have produced storms with anomalous charge structure varied from region to region

Correspondence to:
D. R. MacGorman,
don.macgorman@cox.net

Citation:
Eddy, A. J., MacGorman, D. R., Homeyer, C. R., & Williams, E. (2021). Intraregional comparisons of the near-storm environments of storms dominated by frequent positive versus negative cloud-to-ground flashes. *Earth and Space Science*, *8*, e2020EA001141. https://doi.org/10.1029/2020EA001141

Received 29 APR 2020
Accepted 18 FEB 2021

Abstract We gridded 11 years of cloud-to-ground (CG) flashes detected by the U.S. National Lightning Detection Network during the warm season in 15 km × 15 km × 15 min grid cells to identify storms with substantial CG flash rates clearly dominated by flashes lowering one polarity of charge to the ground or the other (+CG flashes vs. −CG flashes). Previous studies in the central United States had found that the gross charge distribution of storms dominated by +CG flashes included a large upper negative charge over a large middle level positive charge, a reversal of the usual polarities. In each of seven regions spanning the contiguous United States (CONUS), we compared 17 environmental parameters of storms dominated by +CG flashes with those of storms dominated by –CG flashes. These parameters were chosen based on their expected roles in modulating supercooled liquid water content (SLWC) in the updraft because laboratory experiments have shown that SLWC affects the polarity of charge exchanged during rebounding collisions between riming graupel and small ice particles in the mixed phase region. This, in turn, would affect the vertical polarity of a storm's charge distribution and the dominant polarity of CG flashes. Our results suggest that the combination of parameters conducive to dominant +CG flash activity and, by inference, to anomalous storm charge structure varies widely from region to region, the lack of a favorable value of any particular parameter in a given region being offset by favorable values of one or more other parameters.

Plain Language Summary The warm rising wind which creates a thunderstorm sometimes produces unusually large amounts of small liquid water droplets at temperatures less than 0°C. The amount can be enough to produce positive charge in the middle regions of the storm and negative charge in the upper regions, reversing the usual vertical order. Lightning strikes in these unusual storms typically lower positive charge to ground instead of the usual negative charge. We analyzed 11 years of cloud-to-ground lightning flash data from the U.S. National Lightning Detection Network to identify individual storms in which very high or very low percentages of lightning strikes lowered positive charge to the ground. We then compared the environments of the two types of storms. Various combinations of environmental characteristics expected to enhance the amount of liquid droplets at temperatures less than 0°C were associated with storms having lightning strikes dominated by flashes that lowered positive charge to ground, but the specific combination varied from one region to another. We infer, therefore, that the environmental conditions causing the unusual vertical arrangement of thunderstorm charge often associated with these positive flashes also varies. No environmental property that we evaluated appeared to be important in all regions.

1. Introduction

In this study, what we wanted to do was to investigate the environments across the contiguous United States (CONUS) that are conducive to producing storms with charge distributions having an inverted vertical polarity, with positive charge at middle levels (roughly −10°C to −20°C) where negative charge typically is observed and negative charge at upper levels (roughly −40°C to −50°C) where positive charge typically is observed. That warm-season storms can have such a charge distribution was first demonstrated definitively by the Severe Thunderstorm Electrification and Precipitation Study (STEPS) in northwestern Kansas, southwestern Nebraska, and northeastern Colorado in 2000 (Lang et al., 2004; Rust et al., 2005; Rust &

MacGorman, 2002). Such storms have been observed in relatively few other regions (e.g., Fuchs et al., 2015), and we wanted to investigate whether conditions that have been suggested as conducive to these storms in these regions apply more generally. Unfortunately, definitive observations of inverted-polarity storms exist only in the few regions already studied in the literature, so we sought a less direct approach.

We based our indirect approach on results from the STEPS field project. A major goal of STEPS was to determine what storm characteristics were responsible for producing storms in which most cloud-to-ground (CG) flashes lower positive charge to ground (+CG flashes) instead of the usual negative charge (−CG flashes), itself an unexpected observation made possible by the advent of networks for automatically mapping lightning ground strikes that lowered either polarity of charge to ground (e.g., Krider et al., 1980; MacGorman & Taylor, 1989; Orville, 2008): Although <10% of CG flashes in most regions of the CONUS are +CG flashes, rather than the usual −CG flashes (e.g., Boccippio et al., 2001; Orville & Huffines, 2001), most of the cloud-to-ground lightning produced by some warm-season storms are +CG flashes (Branick & Doswell, 1992; Curran & Rust, 1992; MacGorman & Burgess, 1994; Reap & MacGorman, 1989; Seimon, 1993; Smith et al., 2000). A definitive explanation for these anomalous storms was initially difficult to establish, however, because such storms are rare in most regions and establishing an explanation required in-storm soundings of the electric field with concurrent four-dimensional maps of in-cloud lightning, a combination unavailable in regions typically producing such storms until almost 2000. The STEPS region was selected for intensive study because it had an unusually large rate of +CG flashes (e.g., Boccippio et al., 2001; Lang et al., 2004; Orville & Huffines, 2001). What was found was that STEPS storms in which most CG flashes were +CG flashes all had inverted-polarity vertical charge distributions (MacGorman et al., 2005; Rust et al., 2005; Tessendorf, Rutledge, Weins, 2007; Tessendorf, Wiens, Rutledge, 2007; Weiss et al., 2008; Wiens et al., 2005).

An obvious question then was: What environments produce storms with anomalous charge distributions? As described in following sections, studies of storms with anomalous charge distributions have offered a number of hypotheses for the environmental processes responsible for producing these storms, but these explanations have focused mainly on storms in the STEPS region or in Oklahoma and north Texas. All of these hypotheses have involved processes that enhance supercooled liquid water content (SLWC) in the presence of riming graupel because laboratory studies (e.g., Emersic & Saunders, 2010; Jayaratne et al., 1983; Saunders & Peck, 1998; Takahashi, 1978; Takahashi & Miyawaki, 2002) have found that unusually large concentrations of SLWC cause graupel in the mixed-phase region to gain positive charge during rebounding collisions with smaller ice particles regardless of temperature.

Because all storms in STEPS in which +CG flashes dominated CG activity had anomalous charge distributions, two previous studies that examined environmental influences on the polarity of charge distributions used data from the National Lightning Detection Network (NLDN; Cummins & Murphy, 2009; Orville, 2008) in Oklahoma, Kansas, and the Texas panhandle (Carey & Buffalo, 2007) or in the STEPS region (Lang & Rutledge, 2011) to identify storms in which +CG flashes constituted an unusually large fraction of their CG activity. Like them, the present study identifies suitable storms in the NLDN data to examine a broad range of environmental influences, but it broadens the scope of previous studies by analyzing storms across the whole of CONUS. At a minimum, this is the first CONUS-wide climatological study of storms in which +CG flashes constitute a large percentage (≥80%) of frequent CG flashes detected by the NLDN. Our inference, supported by the studies mentioned above in the central United States, is that storms with large +CG percentage thresholds have inverted-polarity vertical charge structure. This inference needs to be verified eventually in other regions, as there is a lack of internal storm soundings with electric field measurements characteristic of inverted-polarity charge structure in storms outside of the central CONUS.

The criteria we chose for including storms in our study were intended to focus on deep convective cells during the warm season and to eliminate or minimize the influence of other storm scenarios in which CG activity can be dominated by +CG flashes, such as winter storms and the stratiform region of mesoscale convective systems, which are influenced by different environmental parameters. Environmental data were acquired from the North American Regional Reanalysis (NARR) data set (Mesinger et al., 2006; NCAR/UCAR, 2020). The environmental parameters analyzed in our study were suggested by previous studies as possibly influencing supercooled liquid water content enough to invert the polarity of a storm's vertical charge distribution, as will be described in later sections.

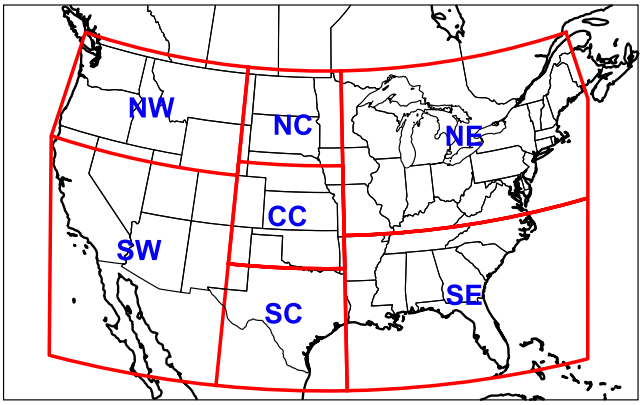

Figure 1. Boundaries of the analysis domain and the regions for evaluating environmental parameters favorable for +CGs. The analysis domain is bounded in red. The CONUS and surrounding regions are divided into seven regions whose boundaries are also shown in red: southwest (SW), northwest (NW), southcentral (SC), central-central (CC), northcentral (NC), southeast (SE), and northeast (NE). CONUS, contiguous United States.

2. Data and Methods

2.1. Lightning Data

All CG flash data from the years 2004–2014 were obtained from Vaisala's NLDN (Cummins & Murphy, 2009). We chose this analysis period in order to ensure consistent network specifications, as it spanned the period between two major upgrades to the NLDN, one from 2002 to 2003 (Cummins & Murphy, 2009) and one in August 2015 (Nag et al., 2016). All flashes were gridded onto a 15 km × 15 km × 15 min Cartesian grid spanning the CONUS using a Lambert Conformal conic projection (Snyder, 1987). The standard parallels chosen for the projection were 33°N and 45°N in order to minimize areal distortion across the CONUS (Alpha & Snyder, 1982). The grid was centered about a reference longitude of −95.8°E because this was the average of the westernmost and easternmost longitudes of our analysis domain. The analysis domain is shown in Figure 1.

We chose to grid only those +CG and −CG flashes estimated by the NLDN to have peak current magnitudes ≥15 kA, intending to remove most misclassified cloud pulses while not discarding too many real CG flashes as would occur if we had chosen a higher threshold. Testing by the University of Arizona after the 2002–2003 NLDN upgrade showed that close to 90% of events with peak currents less than 10 kA that were interpreted as +CG flashes were actually misidentified cloud pulses (Cummins & Murphy, 2009). A similar situation was found for intracloud flashes (ICs) misidentified as −CG flashes in inverted-polarity storms (Calhoun et al., 2013; Fleenor et al., 2009). Because we intended to focus on inverted-polarity storms, we adopted the 15 kA threshold for both polarities of CGs.

Note that some of the +CG flashes tabulated in our data set with this threshold are still likely misidentified cloud processes, but misidentifications are unlikely to invalidate our data set of large numbers of storms with significant CG flash rates in which +CGs comprised ≥80% of CG flashes. Although Leal et al. (2019) found that the NLDN misclassified some compact intracloud discharges (CIDs) in Florida as large peak current +CGs, the data set used in that study was from 2016, when major instrumentation and central processing changes caused many false +CG detections for a couple of years (Murphy et al., 2020). Furthermore, Leal et al. (2019) did not address the reverse relationship, the fraction of NLDN-detected +CGs that were actually intracloud processes, and previous studies suggest that this relationship is manageable in analyses of a large data base. For example, a study evaluating a still older generation of NLDN technology in Oklahoma (MacGorman & Taylor, 1989) than used in this study found that >90% of +CG flashes and −CG flashes with peak currents greater than approximately 15 kA had ELF return-stroke signatures verifying they were CG flashes. The percentage was slightly lower for peak currents >35 kA, but was still approximately 90% for −CGs and only a couple of percentage points lower for +CGs. In a video study of +CGs detected in normal-polarity storms by the same version of the NLDN as used in this study, Biagi et al. (2007) found that the percentage of +CG strokes with peak currents >20 kA that had a verified channel to ground ranged from 67% to 95% in the storms they observed in north Texas and southern Oklahoma. Fleenor et al. (2009) analyzed +CGs detected mostly from inverted polarity storms in the CC region, again by the same NLDN version. Using video recordings and broadband electric field waveforms from the Los Alamos Sferic Array (LASA, Shao et al., 2006), they found that only one out of more than 1,000 +CG strokes detected by the NLDN with a peak current >20 kA was actually due to an intracloud process. From the data used in these studies, Murphy et al. (2020) indicated that 13% of +CG strokes detected by the NLDN with peak currents ≥15 kA after the 2003 upgrade were actually misidentified intracloud processes.

Initially grid cubes were constructed every 5 km in the *x*- and *y*-directions and every 5 min in time. For our analysis, however, we chose grid cell dimensions of 15 × 15 km by 15 min based on the typical spatiotemporal characteristics of an individual storm cell and constructed these larger grid cells by stepping forward every 5 km in *x* and *y* and every 5 min in time in order to determine the time and location of local maxima in

flash counts with higher resolution. Grid cells were included in the analysis only if they had ≥10 CG flashes, ≥80% of which were +CGs, or if they had ≥20 CG flashes, ≥90% of which were −CGs. The cells in the former (latter) group were inferred to be associated with inverted- (normal-) polarity electrical charge structure in the corresponding storm cell. Thresholds were made larger for cells dominated by −CG flashes to reduce the number of −CG dominated cells, but the remaining number was still more than an order of magnitude larger overall than the number of +CG dominated cells.

Because the intended focus of this study is on deep convective storm cells having inverted-polarity vertical charge structure, we attempted to minimize the influence of +CG flashes that can dominate CGs in many winter storms (e.g., Engholm et al., 1990; Orville et al., 1987; Rudlosky & Fuelberg, 2011; Takagi et al., 1986; Takeuti et al., 1978) or in the stratiform region of many mesoscale convective systems (e.g., MacGorman & Morgenstern, 1998; Makowski et al., 2013; Rutledge et al., 1993; Rutledge & MacGorman, 1988; Williams et al., 2010) by restricting our analysis in three ways: (1) We included data only from the warm season (defined below based on the region of the CONUS in which the cell was located). (2) Because MCSs tend to grow upscale from earlier convective storms and stratiform regions tend to peak starting around midnight (Maddox et al., 1986), we included only grid cells that occurred between 15:00 and 23:00 local time to attempt to minimize the impact of +CG-dominated grid cells from stratiform regions. (3) Because flash rates in an arbitrary 15 × 15 km stratiform region of an MCS are typically small, we chose a substantial total CG flash rate threshold of 10 per 15 min for +CG flash rates.

Once the +CG- and −CG-dominated cells had been identified and the above filtering had been applied, the spatial and temporal overlap among grid cells was removed in order to reduce the amount of sample interdependence. This was carried out by ordering all grid cells from the greatest to least number of CG flashes and by working down the list cell by cell to eliminate cells that occurred within 15 km in space on all sides and within 30 min in time of the cell being considered (these thresholds may have eliminated some storm cells that were actually separate).

2.2. Environmental Data

Once the data set of +CG- and −CG-dominated cells had been built, environmental data from the NARR data set (Mesinger et al., 2006; NCAR/UCAR, 2020) were linked to each cell. The NARR provides data on 45 vertical levels on a 32 km × 32 km × 3 h grid, from 1979 to the present. We extracted 17 of the environmental parameters which various previous studies have analyzed and divided them into three categories: moisture parameters, dynamic parameters, and thermodynamic parameters as follows:

- *Moisture parameters*
  Dew point depression (DPD) at 2 m AGL, cloud base height (CBH), warm-cloud depth (WCD), and precipitable water (PWAT).
- *Thermodynamic parameters*
  Surface equivalent potential temperature (θ_e), convective available potential energy (CAPE) from the level of free convection (LFC) to the equilibrium level (EL), normalized CAPE from LFC to EL (NCAPE, i.e., CAPE divided by the distance between these two reference levels), LFC to −20°C CAPE, LFC to −20°C NCAPE, 0°C to −20°C CAPE, 0°C to −20°C NCAPE, convective inhibition (CIN), and EL altitude.
- *Dynamic parameters*
  0–3 km wind shear, 0–6 km wind shear, 0–3 km storm-relative helicity (SRH), and storm-relative wind speed at the EL.

The way in which each parameter has been hypothesized to affect SLWC is described in later sections as the analysis of each parameter is presented and again in the discussion section. Although some parameters are highly correlated with each other, we included them partly to see if minor variations caused different impacts and partly as a sanity check on the results of our statistical analysis.

It should be noted that the NARR does not directly assimilate surface temperature or dew point temperature. However, it does assimilate radiosonde data aloft and close to the surface. The CAPE parameters were not taken directly from the NARR but were instead calculated by the authors from the appropriate parameters provided directly by the NARR. Parcel ascent was assumed to begin at the higher of 1,000 hPa or 10 hPa

Table 1
Sample Sizes for Each Parameter & Each Region for the +CG- (−CG-) Dominated Cells With at Least 10 (20) Flashes in 15 min & at Least (at Most) 80% (10%) +CG Flashes

	SW	NW	SC	CC	NC	SE	NE
WCD and CBH	1,494 (39,891) 3.6%	528 (5,112) 9.4%	1,321 (58,380) 2.2%	14,006 (45,909) 23.4%	11,170 (7,874) 58.7%	1,148 (205,020) 0.56%	4,287 (116,150) 3.6%
All other parameters	1,581 (41,472) 3.7%	639 (6,254) 9.3%	1,644 (62,023) 2.6%	16,640 (50,098) 24.9%	13,580 (9,473) 58.9%	1,207 (207,640) 0.58%	4,812 (119,460) 3.9%

Note. The bottom parameter is the percentage of storm cells analyzed in each region that were +CG-dominated cells.
Abbreviations: CBH, cloud base height; CC, central-central; NC, northcentral; NE, northeast; NW, northwest; SC, southcentral; SE, southeast; SW, southwest; WCD, warm-cloud depth.

above the lowest NARR level located above the surface ("hybrid level 1"). See Eddy (2018) for more details on how the CAPE parameters and other parameters were calculated. It should also be noted that CBH was taken directly from the NARR. The NARR obtains CBH by taking the lowest level above the surface at which the cloud water/ice mixing ratio is greater than 10^{-6} kg kg^{-1}. If no clouds are inferred by this method, the NARR algorithm checks for any convective clouds and returns their CBHs (An et al., 2020).

Due to its coarse resolution, we linearly interpolated in time and used the closest possible NARR grid point in space to obtain the values of each environmental parameter as close as possible to the time and location of each storm cell. Sometimes the characteristics of the environment interpolated from the NARR did not match characteristics that would be required to produce a cell with vigorous electrical activity. For example, some cells occurred at NARR grid points with 0 J kg^{-1} of CAPE from the LFC to EL. This could have also been the result of the storm itself affecting its nearby environment. To preserve only those cases in which the environment seemed less affected by nearby storm cells or in which interpolation did not lead to counterintuitive values, only those cells with an EL of at least 7 km were kept.

The CONUS was partitioned into seven regions: the southwest (SW), northwest (NW), southcentral (SC), central-central (CC), northcentral (NC), southeast (SE), and northeast (NE) regions (Figure 1); and the environmental parameters of +CG-dominated cells were compared with those of −CG-dominated cells within each region. The warm season was defined to be April–October in the SW, SC, and SE regions and from May to September in the other regions. This is the first study to compare the environmental differences favoring +CG production between these two categories of CG cells within each of several regions spanning the entire CONUS. Additionally, no other study has used +CG threshold percentages this high for +CG dominated cells and +CG threshold percentages this low for −CG dominated cells to distinguish cells with many +CG flashes from cells with few +CG flashes. Besides giving a climatology of +CG-dominated cells, we expect that the more extreme threshold percentages that we use here will better elucidate those environmental characteristics favorable for producing cells with anomalous charge structures, although that remains to be verified in regions outside the CC region, which has already been analyzed. The sample sizes of +CG- and −CG-dominated cells for every region and environmental parameter are shown in Table 1. Overall, approximately 7.5% of the cells analyzed in the study were +CG-dominated.

For each region and every environmental parameter, we determined the distribution of the values of the parameter for +CG-dominated cells and for −CG-dominated cells. Note that variations in climatological conditions within the individual regions probably affected our distributions, but regions needed to be fairly large to provide enough samples for our statistical analysis. We then conducted a permutation test (Wilks, 2011) to analyze whether the difference in median values for the two distributions was statistically significant. The test was two-tailed because we did not know *a priori* whether the median value of the parameter for the +CG-dominated cells would be greater or less than that for the −CG-dominated cells. The null hypothesis was that the two medians were not truly different in that region. For a given region and parameter, we performed the test by taking the full sample set of the smaller of the two sets (usually the +CG-dominated cells) and an equal number of samples of the larger sample set chosen at random. After combining these two groups into one group, half of the group was chosen at random, and the median value

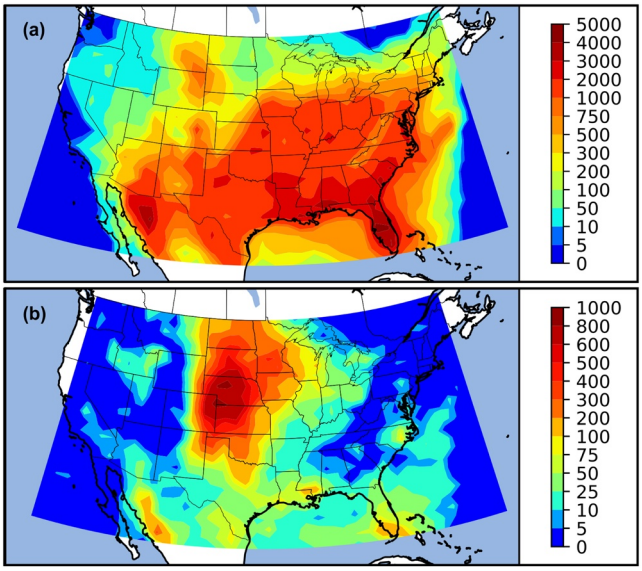

Figure 2. Number per 15 × 15 km area of (a) −CG dominated cells, inferred to have normal-polarity charge structure and (b) +CG dominated cells, inferred to have inverted-polarity charge structure from 11 years of warm-season NLDN data, after the filtering described in Section 2. Note that the color scale used is logarithmic, and each contour is labeled on the color bar. NLDN, National Lightning Detection Network.

of the parameter for that group and the median value for the remaining group were both calculated. The difference between these two median values was then the value for one trial. The above steps were repeated for different randomly chosen groups for a total of 10,000 iterations, from which a null distribution of differences in the medians was generated. Then, the actual difference in medians of the two original unreduced samples was compared with the null distribution to calculate the significance level of the difference. Because the test was two-tailed (i.e., the actual difference in medians could be either less than or greater than the median of the null distribution), the calculated probability p that the null hypothesis was true is given by $p = 2n$, where n is the smaller of (1) the fraction of median differences in the null distribution greater than the actual difference or (2) the fraction of median differences in the null distribution less than the actual median. The difference in two medians is considered statistically significant (i.e., the null hypothesis is considered false) at a level S (in percent) if $p < 1 - S / 100$. For an observed difference between +CG and −CG medians to be considered statistically valid at a level ≥95% then meant that the value of p obtained by comparing the actual difference in the two medians with the null distribution accumulated from our 10,000 trials must be <0.05.

Besides the p value for each parameter and region, we determined two other parameters:

1. We computed the percent difference in the median parameter values for +CG- and −CG-dominated cells as $100*(\text{median}_{(+CG)} - \text{median}_{(-CG)})/[0.5*(\text{median}_{(+CG)} + \text{median}_{(-CG)})]$
2. Besides the percent difference, which measures the difference in medians relative to the average of the median parameter values, a reviewer requested that we provide a measure of the effect size of the difference in medians given by Cohen's d (Cohen, 1988; Cumming, 2012), defined as the magnitude of the difference in median values divided by the pooled standard deviation of the two parameters. This would have required us to compute the standard deviations of all 238 distributions (2 times 17 times 7), but we did not have access to our data sets during the COVID-19 pandemic and so could not do that. However, we did have the inner quartile ranges (IQR = 75th percentile − 25th percentile) from violin plots for all 17 parameters, including the 10 parameters shown in violin plots in later sections, and so defined an analogous statistic which measures the difference in medians in units of the pooled IQR instead of the pooled standard deviation. A method analogous to one used for the pooled standard deviation gives the pooled IQR as $\{0.5*[(IQR_{+CG})^2 + (IQR_{-CG})^2]\}^{1/2}$. Mimicking Cohen's d, we call the resulting statistic the effect size of the parameter. To describe the effect size in broad categories, we somewhat arbitrarily defined the following ranges: large, ≥0.45; moderate, ≤0.44 and ≥0.30; small, ≤0.29 and ≥0.15; and very small, ≤0.14

3. Geographic Distribution of –CG and +CG-Dominated Cells

Figure 2a shows the geographic distribution of –CG-dominated cells (≥20 flashes in 15 min, ≥90% being −CG flashes) across the CONUS. Much as for climatologies of –CG flashes and of total CG flashes (e.g., Medici et al., 2017; Orville & Huffines, 2001), there is an overall increase in the number of storm cells roughly from the NW to the SE, with the highest concentrations located in central Florida. This similarity is expected because roughly 90% of CG flashes in the CONUS are −CG flashes (Cooray, 2015). Figure 2b shows the distribution of +CG-dominated cells (≥10 flashes in 15 min, ≥80% being +CG flashes) across the CONUS. These cells are most commonly in the western High Plains region, which is also where inverted-polarity cells have been observed most frequently by studies (e.g., Fuchs et al., 2015; Lang & Rutledge, 2011; MacGorman et al., 2005; Rust & MacGorman, 2002; Rust et al., 2005; Tessendorf, Wiens, & Rutledge, 2007; Tessendorf, Wiens, & Rutledge, 2007; Weiss et al., 2008; Wiens et al., 2005). Additionally, the local maxima in eastern Louisiana/southern Mississippi, southern Florida (also noted there by Marchand et al., 2019),

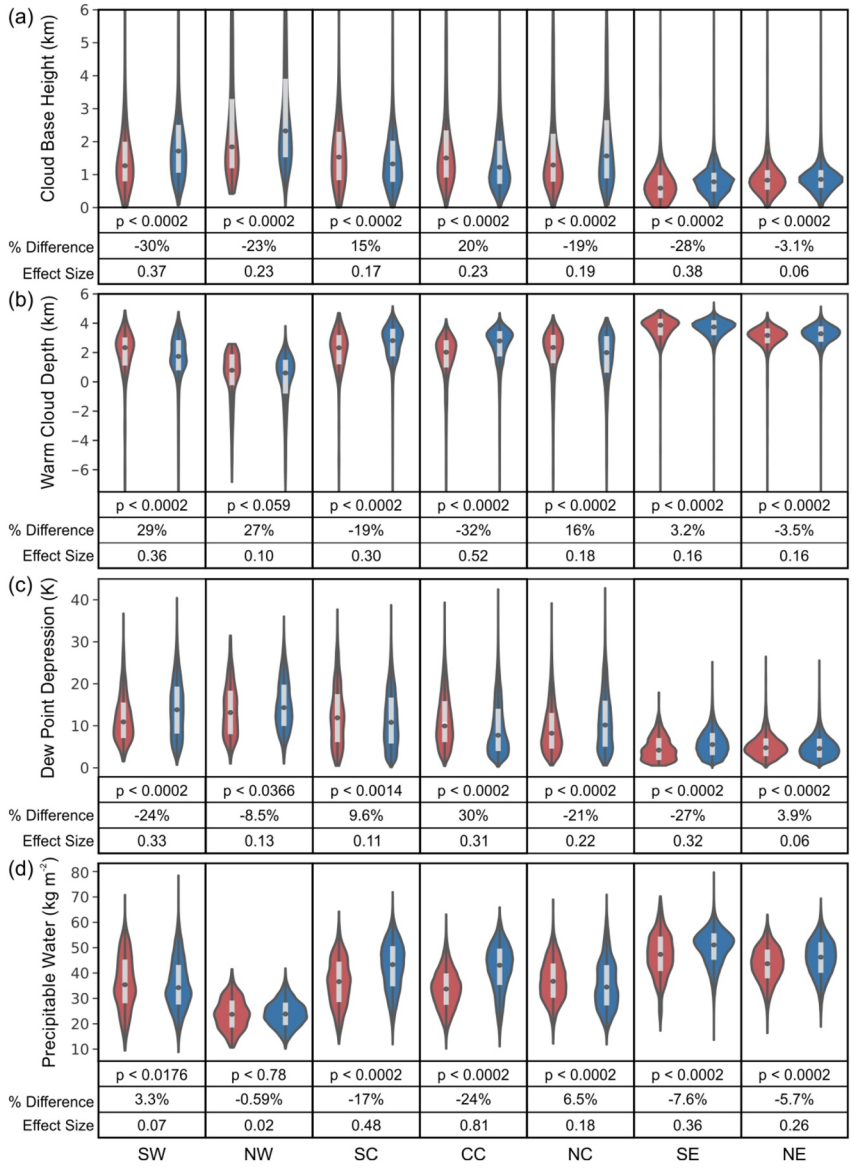

Figure 3. Violin plots of the moisture variables: (a) cloud base height, (b) warm cloud depth, (c) dew point depression, and (d) precipitable water for each region. Each violin plot is scaled such that all violins for a given variable have the same area, and the number of cells with a particular value of the given parameter is proportional to the width of the violin at that value. Red (blue) violins correspond to the +CG- (−CG-) dominated cells. See text for additional explanation.

eastern North Carolina, and in northwestern Mexico indicate the possible presence of inverted-polarity storm cells in those regions, although this has not yet been verified by independent storm-scale observations. Note that the larger +CG cell counts in Kansas, Nebraska, and the Dakotas correspond approximately to a trough of relative minima in −CG cell counts.

4. Differences in the Environments of +CG-Dominated and −CG-Dominated Cells

The sections below show differences in median values of four moisture parameters: CBH, WCD, DPD, and PWAT (Figure 3); three thermodynamic parameters: LFC to EL CAPE, LFC to −20°C CAPE, and CIN (Figure 4); and three dynamic parameters: 0–6 km shear, storm-relative wind speed at the EL, and SRH

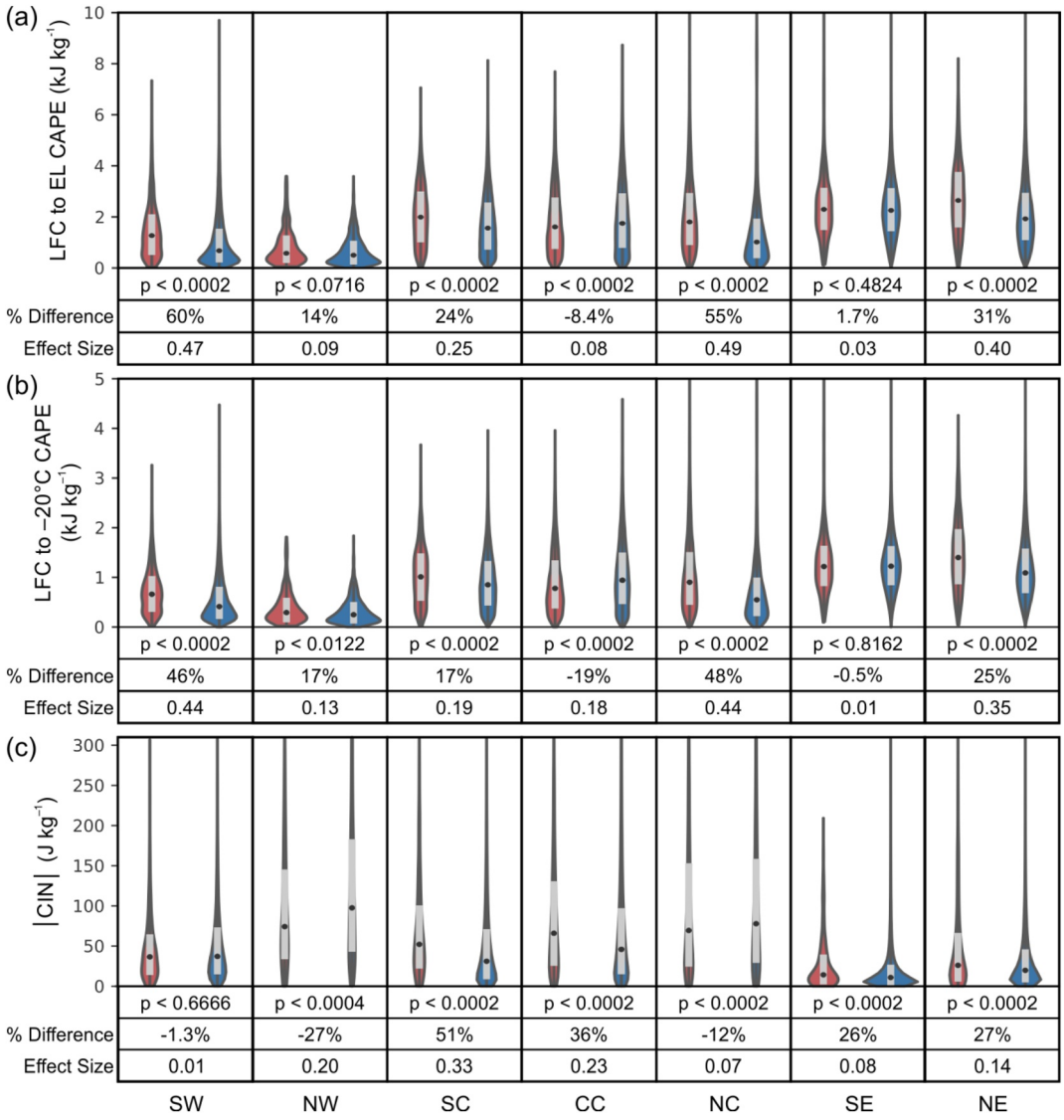

Figure 4. Violin plots of the thermodynamic variables: (a) LFC to EL CAPE, (b) LFC to −20°C CAPE, and (c) |CIN| for each region. Red (blue) violins correspond to the +CG- (−CG-) dominated cells. See text and caption for Figure 3 for more explanation of the figure.

(Figure 5), between the two types of cells in each of the seven regions spanning the CONUS. Special emphasis will be placed in our discussion on the CC and NC regions because these two regions have a greater sample size of +CG-dominated cells than all of the other regions combined (Table 1). Furthermore, environmental controls on storm polarity have previously been studied more in the CC region than in any other region.

The distribution of values for each of these parameters is shown by violin plots for the two types of cells for each region. The width of the violin shape at a given value of a parameter is proportional to the number of storm cells having that value, normalized so that all violin plots have the same total area. The distributions for +CG (−CG) dominated cells are colored in red (blue). Box-and-whisker plots are overlaid on the violins. The bottom of the light gray box indicates the 25th percentile, the black circle within the gray box indicates the median value, and the top of the gray box indicates the 75th percentile. Below each +CG and −CG pair of violin plots are three statistical measures of the difference in medians for the pair, as described in Section 2. *p*-Values were determined from a two-tailed permutation test. Each *p*-value can be multiplied by 100 to yield the probability (in percent) of achieving the given difference in medians if there were truly

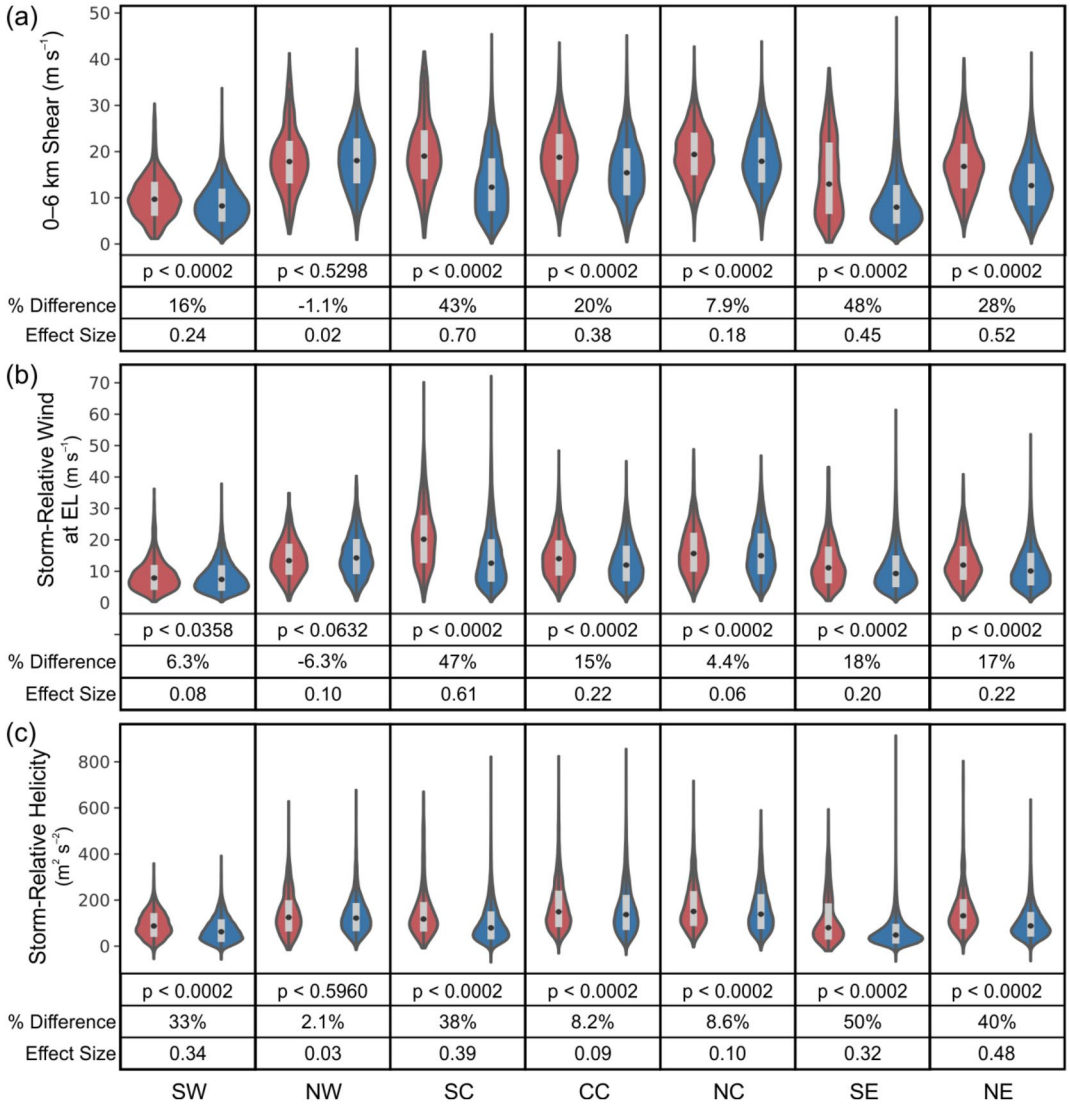

Figure 5. Violin plots of the dynamic variables: (a) 0–6 km shear, (b) storm-relative wind speed at the equilibrium level, and (c) storm-relative helicity for each region. Red (blue) violins correspond to the +CG- (−CG-) dominated cells. See text and caption for Figure 3 for more explanation of the figure.

no difference in the two populations of cells. Thus, a low *p*-value indicates that the median values of the parameter for +CG- and −CG-dominated cells are likely different, with a significance level $S = 100*(1 - p)$. The percent difference and effect size of the medians of the two distributions are also shown below the corresponding violin plots; a positive value indicates that the median value for the +CG-dominated cells was greater.

4.1. Moisture Parameters

4.1.1. Cloud Base Height

Williams et al. (2005) and Fuchs et al. (2015) suggested that higher CBHs increase SLWC in the updraft by decreasing the warm cloud depth (WCD) and, therefore, could contribute to shorter warm cloud residence time. They also indicated that storms with higher CBHs tend to have broader, stronger updrafts, so the water content would be less diluted by dry-air entrainment in their updraft core and more water content would be transported to the mixed-phase region in the core. Figure 3a shows the distribution of CBHs

for +CG-dominated cells and for −CG-dominated cells. All regions had a significant difference in median CBHs, with $p < 0.0002$ (i.e., were significantly different at the 99.98% level).

The SC and CC regions were the only regions with higher median CBHs in +CG-dominated storms than in −CG-dominated storms, and even in these two regions, two other moisture parameters had a much larger effect size (Figure 3). The region containing cells with the highest median CBH for +CG-dominated cells was the NW region, but this region had the smallest sample size of +CG-dominated cells, and its median CBH for −CG-dominated cells was even higher. It seems contrary to the expectations of Williams et al. (2005) that the hypothesized relationship with CBH did not hold in the NC region, which had the second-highest sample size of +CG-dominated cells, although we shall see that their suggested role of superlative updrafts will be supported by other parameters analyzed in this paper. The fact that the median CBH was higher for −CG-dominated storm cells in all regions except the SC and CC regions suggests that the hypothesized role of CBH is not the only factor that can cause a cell's CGs to be dominated by +CGs, although it appears to have contributed in the SC and CC regions.

4.1.2. Warm Cloud Depth

While CBH influences WCD by providing its lower boundary, the height of the 0°C isotherm provides its upper boundary, so WCD's influence may differ from that of CBH. A shallower WCD is a candidate for allowing higher SLWCs by decreasing the warm cloud residence time of parcels ascending in the updraft (e.g., Carey & Buffalo, 2007; Fuchs et al., 2015; Williams et al., 2005). Figure 3b shows the distribution of WCD in +CG- and −CG-dominated cells for all regions. In all regions except for the NW region, the difference in median WCD was significant at the 99.98% level. It was significant at the 94.1% level in the NW region, below our 95% level threshold. A negative value of WCD meant that the cloud base was above the freezing level.

+CG-dominated cells in the CC region were found to have a median WCD that was 28% shallower than the region's −CG-dominated cells, but in the NC region +CG-dominated cells had a median WCD that was 19% deeper than −CG-dominated cells. The regions in which +CG-dominated cells had shallower WCDs were the SC, CC, and NE regions, although the percent difference and effect size in the NE were very small. In the CC region, WCD had a large effect size. Its effect in two adjoining regions was smaller, a moderate effect size in the SC and a much smaller effect size in the NE.

In the remaining regions, median WCD was greater for +CG-dominated cells than for −CG dominated cells, although the percent difference was small in the SE. The NW region, which had the shallowest median WCD for +CG-dominated storms compared to any other region, had an even shallower median WCD for −CG-dominated storms. The fact that the median WCD for +CG-dominated storms was greater than the median for −CG-dominated storms in a majority of regions suggests that WCD is not by itself a sufficient factor for determining the polarity of a storm's charge distributions and the dominant polarity of its CGs.

4.1.3. Dew Point Depression

Several early studies found that supercell storms dominated by +CG flashes tended to occur in drier subcloud regions with larger DPDs (Knapp, 1994; MacGorman & Burgess, 1994; Smith et al., 2000), so our environmental analysis of DPD was intended to test whether this was generally true. Furthermore, DPD and CBH can be approximated to scale linearly with one another (Williams et al., 2005), so we would expect higher DPDs to favor greater SLWCs in a way similar to the influence hypothesized for CBH. Figure 3c shows the distribution of DPD in the environments of −CG- and +CG-dominated cells for all regions. The difference between the median DPD of +CG-dominated cells and that of −CG-dominated cells was significant at >95% in all regions.

As one might expect, the regions in which the median difference in DPD was positive and, therefore, was hypothesized to favor +CGs, were the same as those in which WCD also was consistent with the +CG hypothesis: Only the CC, SC, and NE regions each had a positive percent difference in medians, although the difference was small in the NE. At 35%, the CC region had the largest difference in median DPDs favoring +CG-dominated cells, but two other moisture parameters had much larger effect sizes in that region. However, as with the trend for CBHs and WCDs, the DPDs in the SE, NC, SW, and NW regions actually had negative differences in median DPDs, which meant that −CG-dominated cells had larger median DPDs than +CG-dominated cells had and, therefore, would have been hypothesized to tend toward having less

SLWC in the +CG dominated cells, a fact which argues again that larger DPD alone is insufficient for producing +CG-dominated storms.

4.1.4. Precipitable Water

As for the other moisture parameters, we analyzed PWAT because Carey and Buffalo (2007) suggested that lower PWAT maximizes SLWC by reducing water loading in the updraft, which would suppress the collision-coalescence processes that act to deplete the smaller cloud droplets that contribute to the SLWC and reduce the entrainment of dry air, allowing more liquid water to ascend into the mixed-phase region. Furthermore, reduced water loading in the updraft could allow stronger updrafts for the same amount of CAPE. The resulting reduced transit times for depleting SLWC below the mixed-phase region would allow a larger fraction of the liquid water to ascend into the mixed-phase region. If a lower PWAT has this effect, we would expect a tendency for +CG-dominated cells to have lower PWAT. Figure 3d shows the distribution of PWAT in −CG- and +CG-dominated cells for all regions.

The differences in the medians were significantly different at a level ≥ 98% in all regions except in the NW region, where the medians were not significantly different. PWAT had an effect of the appropriate sign in more regions than the other moisture parameters, having among the largest effect sizes in the SC and CC regions, a moderate effect size in the SE, and a small effect size in the NE. It was the only moisture parameter having an effect consistent with the hypothesized sign in the SE. Note, however, that the SW and NC regions both had a difference in median values deemed unfavorable for producing +CG-dominated cells for all of the moisture variables, and the NC region had the second largest number of +CG-dominated cells. Thus, while PWAT may contribute to producing +CG-dominated cells (presumably having inverted-polarity charge distributions) in some regions, the fact that there were exceptions suggests that PWAT, like the other moisture variables, is not sufficient alone; other types of environmental parameters (e.g., thermodynamic or dynamic) need to have favorable values in at least some situations.

4.2. Thermodynamic Parameters

4.2.1. LFC to EL CAPE

The hypothesis being tested here is that, even if warm cloud depths were larger than optimal values, greater updraft speeds would reduce the warm cloud residence time needed for precipitation growth in an ascending air parcel and so might enhance the amount of SLWC enough to produce an inverted-polarity charge distribution (e.g., Fuchs et al., 2018, 2015; Williams et al., 2005). Figure 4a shows the distribution of LFC to EL CAPE in +CG- and −CG-dominated cells for all regions. The difference in median values was statistically significant at the 98.98% level in the SW, SC, CC, NC, and NE regions, but was not statistically significant at the 95% level in the NW and SE regions.

In all regions except the CC region, +CG-dominated cells had larger median values of LFC to EL CAPE than −CG-dominated cells had. In the SW and NC regions, this CAPE parameter had the largest favorable effects and percent differences favoring +CGs, yet Figure 3 showed that in these two regions differences in median values for the moisture category of parameters uniformly favored −CG-dominated cells rather than +CG-dominated cells. Thus, it appears that the additional LFC to EL CAPE needed to produce +CG-dominated storms was especially great in the SW and NC regions. The effect size was moderate in the NE, small in the SC, and very small in the SE. The environment of cells of both polarities in the NW region had lower median LFC to EL CAPE than in other regions, and this may help explain why the NW region had the fewest observations of cells dominated by either polarity of CG flashes.

4.2.2. CAPE From the LFC to −20°C

CAPE through the layer from the LFC to −20°C considers the effect of updraft speed in the middle of the mixed-phase region rather than considering the whole depth of the storm. Figure 4b shows the distributions of LFC to −20°C CAPE in −CG- and +CG-dominated cells for all regions. Much as in the case of LFC to EL CAPE, all the medians were statistically different at ≥98.78% except in the SE region, where the difference in medians was not statistically different.

Once again, it appears clear that no one environmental parameter clearly leads to +CG-dominated or −CG-dominated cells (and by inference, to inverted- or normal-polarity cells). The median LFC to −20°C CAPE was larger for +CG-dominated cells in all regions with statistically significant differences except in the CC region. In the CC region, the median LFC to −20°C CAPE for +CG-dominated cells was 17% smaller than that for −CG-dominated cells; however, as noted previously, all the moisture parameters considered in previous sections tended to be favorable there. In the NC and SW regions, on the other hand, the percent difference and effect size of median LFC to −20°C CAPE were relatively large and second only to LFC to EL CAPE, so this parameter was a good discriminator between the two categories of cells there, although the medians of moisture parameters in those regions were unfavorable for +CG-dominated cells. Note also that the magnitude of the median LFC to −20°C CAPE for +CG-dominated cells was not as important as its value relative to the median for −CG-dominated cells. One of the largest median values for +CG-dominated cells occurred in the SE region, yet the difference between the +CG median and the –CG median in that region was not significantly different.

4.2.3. Convective Inhibition

We analyzed the magnitude of CIN because, all else being equal, shifting the temperature at which a parcel attains free convection to higher temperatures tends to make the storms that do occur more isolated, with less competition for inflowing air and moisture, and thereby to increase the CAPE realized by parcels above the LFC. Thus, storms that do form with larger magnitudes of |CIN| tend to be stronger storms (Fuchs et al., 2018; Rasmussen & Houze, 2016), with stronger updrafts, resulting in shorter warm-cloud residence times and greater supersaturation in the mixed phase region. We hypothesize, therefore, that environments with greater |CIN| are more likely to realize greater SLWC. Figure 4c shows the distributions of |CIN| in −CG- and +CG-dominated cells for all regions. The median values of |CIN| for +CG-dominated and −CG-dominated cells were significantly different in all regions at the 99.96% level or higher except in the SW region, where they were not significantly different.

In the SC and CC regions, |CIN| was the parameter with the largest percent difference supporting the hypothesis regarding +CG-dominated cells, but its effect size was only moderate to small, less than that of several other parameters. |CIN| also supported the hypothesis in the SE and NE regions, where the effect size was small, but did not support it in the NW, NC, and SW regions. The failure of the hypothesis in some regions, particularly in the NC region which had the second largest number of +CG-dominated cells, again means that this parameter cannot solely account for +CG domination. Furthermore, the largest median magnitude of |CIN| was for −CG-dominated cells in the NW, not for +CG-dominated cells there, so again, the absolute median value of |CIN| was not as important as the difference in median values between the two categories of storm cells.

4.3. Dynamic Parameters

4.3.1. 0–6 km Wind Shear

Because stronger 0–6 km shear in horizontal wind is more conducive to rotating updrafts, and updraft rotation causes dynamic pressure gradient forces that can strengthen the updraft (Weisman & Klemp, 1982, 1984), we hypothesized that environments supporting greater 0–6 km shear would support storms with stronger updrafts and therefore shorter warm cloud residence times. Thus, environments with greater 0–6 km shear may tend to have greater SLWCs in the mixed-phase region.

Figure 5a shows the distributions of 0–6 km shear in environments containing −CG- and +CG-dominated cells for all regions. The difference in medians was not statistically significant in the NW region. In all other regions, it was significant at the 99.98% level, and the difference in median values of 0–6 km shear favored higher SLWCs in +CG-dominated cells than in −CG-dominated cells. The percent difference in median 0–6 km shear in each of the three southern regions was larger than the percent difference in each adjoining region north of it, with the two largest magnitudes of percent difference being in the SC and SE regions. The effect size was large in the SC, SE, and NE regions, moderate in the CC region, and small in the SW and NC regions. Note that having a large value of 0–6 km shear was not sufficient in itself to satisfy our hypothesis, as the NW region had relatively large median values, but the difference in medians was not significantly different there.

4.3.2. Storm-Relative Wind Speed at the Equilibrium Level

We calculated storm-relative wind speed at the EL by subtracting the non-pressure-weighted mean of the wind between 0 and 6 km from the wind at the EL. We chose to analyze this parameter because it approximates a parameter suggested to explain the unique characteristics of low-precipitation (LP) supercell storms, and Williams et al. (2005) had noted that the western High Plains, which tends to have more +CG flashes and anomalous charge distributions, also tends to have more LP storms. In a comparison of supercell types, Rasmussen and Straka (1998) found that LP storms had greater upper-level storm-relative winds than other types of supercell storms. They suggested that this caused the precipitation in the anvil to be advected too far for many of the particles to be recirculated back into the updraft core and suggested that this recirculation is necessary to provide seed hydrometeors capable of growing to precipitation size before reaching anvil levels in the roughly 10 min available in typical LP updraft cores. They argued that this is what causes the characteristic observations of LP storms as swirling updrafts made visible by cloud particles without visible precipitation up to roughly anvil levels. Applying this scenario to storm electrification, MacGorman et al. (2011, 2017) suggested that strong anvil-level winds result in fewer precipitation particles in the updraft below the freezing level, as in LP storms, and having fewer precipitation particles available to scavenge cloud droplets through warm-cloud collision-coalescence processes results in larger values of SLWC in the mixed-phase region.

Figure 5b shows the distribution of storm-relative wind speed at the EL in environments containing either +CG-dominated or −CG-dominated cells for all regions. The difference in median values was significant at a level >95% in all regions except the NW, and the median was greater for +CG-dominated cells in all these other regions. The percent difference in median values and the effect size were greatest by far in the SC region, followed by small values in the CC, SE, and NE regions and very small values in the SE and NC regions. Because the median storm-relative wind speed at the EL was not significantly different in the NW region and the percent difference and effect size were very small in two other regions, once again it appears unlikely to be the only important environmental parameter for producing +CG-dominated storms, although it appears to play a role in at least some regions.

4.3.3. 0–3 km Storm-Relative Helicity

We chose to analyze SRH because greater SRH provides greater dynamical forcing of the updraft (Carey & Buffalo, 2007; Weisman & Klemp, 1982) by causing it to rotate, potentially increasing updraft speed due to the dynamic pressure perturbations associated with rotation. Stronger updrafts allow shorter warm-cloud residence times, which increases SLWC because precipitation has less time to collect cloud droplets before entering the mixed phase region. Figure 5c shows the distribution of SRH in environments containing +CG-dominated and −CG-dominated cells in every region. The differences in medians between +CG-dominated and −CG-dominated cells were significant at the 99.98% level in all regions except in the NW region, where the difference was not statistically significant.

The southern regions and the NE had the largest percent differences and effect sizes of medians favoring +CG-dominated cells. The median value of SRH was greater in +CG-dominated cells than in −CG-dominated cells in every region. As for 0–6 km shear, the percent difference in each southern region was considerably larger than the percent difference in the adjoining region north of it and also increased west to east, with the largest percent difference in the east regions. Effect size, however, was large in the NE, was moderate and roughly equal in the SW and SC, and was very small in the CC and NC regions. Again, the fact that the difference was not statistically significant in the NW and that the percent difference and effect size were very small in the CC and NC regions suggests that this parameter is not the only one affecting the dominant polarity of frequent CG flashes (and therefore, inferred to affect the polarity of the charge structure).

4.4. Other Environmental Parameters

In addition to the 10 parameters presented in the above sections, we analyzed equivalent potential temperature θ_e, the equilibrium level (EL), LFC to EL NCAPE, LFC to −20°C NCAPE, 0°C to −20°C CAPE and NCAPE, and 0–3 km shear. NCAPE is CAPE divided by the depth over which it is calculated and gives the average change in CAPE per meter of ascent of an air parcel. Larger values of CAPE, NCAPE, and 0–3 km shear all might increase SLWC by increasing updraft speed within some layer and might thereby reduce

residence time below the middle of the mixed phase region, as discussed previously for other related parameters. θ_e was analyzed because Smith et al. (2000) found that θ_e was smaller in the environments of +CG-dominated storms than in the environments of −CG-dominated storms on analyzed days. EL was chosen because Carey and Buffalo (2007) had found that somewhat lower EL heights were associated with storms in which +CGs constituted relatively high fractions of CG activity (>25% of CGs). If, however, a higher EL is related to greater CAPE, one might expect greater updraft speeds and smaller residence times in the mixed phase region, which might also lead to enhanced +CG production, so we will consider EL in the context of the effect of other parameters, rather than as an isolated parameter.

4.5. Summary of Percent Differences for all Parameters and Regions

The effect size and the percent difference in medians between +CG dominated cells and −CG-dominated cells both are shown for all parameters and regions in Table 2. The following summarizes hypotheses concerning the parameters not discussed in previous sections. More details concerning them are available in Eddy (2018).

Consistent with the findings of Smith et al. (2000) in the CC region, median equivalent potential temperature was smaller for +CG-dominated cells than for −CG-dominated cells in the SC, CC, and SW regions and had moderate effect sizes. All three were regions in which precipitable water was also smaller for +CG cells, with a moderate to large effect size, as discussed previously.

The relationships with the additional CAPE parameters were mixed, but 0°C to −20°C CAPE and NCAPE displayed statistically significant differences between the two types of cells for all regions and favored greater SLWC in the +CG-dominated cells in all regions except the CC region. These two were among the only three parameters favoring greater SLWC in the NW region, and all three were CAPE-related parameters with very small effect sizes. Most CAPE-related parameters had moderate to large effect sizes in four of the seven regions (the SW, SC, NC, and NE regions), and in three of these four regions, moisture parameters were not favorable.

The relationship with EL appeared to depend on relationships with moisture or CAPE parameters: +CG-dominated cells had a smaller median value of EL than −CG-dominated cells had in the SC, CC, and SE regions, consistent with the findings of Carey and Buffalo (2007). These were all regions in which one or more moisture parameters had a moderate to large effect size, so the relationship with EL probably existed for reasons similar to the reasons for the relationships with those parameters. However, +CG-dominated cells had modestly larger median values and moderate to large effect sizes in the SW and NC regions, and the relationships with moisture parameters were inconsistent with the hypothesis for enhanced SLWC in these two regions. However, CAPE parameters associated with greater updraft speeds had large favorable effect sizes in those regions and that likely contributed to the relationship with EL.

The relationship with 0–3 km shear was similar to that of SRH and 0–6 km shear in that median values were higher for the +CG-dominated cells in all regions having significantly different medians. As was true of the other dynamic parameters, the difference in median 0–3 km shear was not significant in the NW region.

5. Discussion and Conclusions

Our goal when designing this study was to determine which environmental parameters are conducive to storms having anomalous vertical charge distributions across all of CONUS. To identify such storms definitively would require some combination of vertical electric field soundings, three dimensional lightning mapping observations, and possibly ground strike mapping systems, such as have been used for studies of individual storms (e.g., Bruning et al., 2010, 2014; MacGorman et al., 2005, 2008; Rust et al., 2005; Wiens et al., 2005) or for regional studies, such as the study of the STEPS region by Lang and Rutledge (2011). However, such observations are available in only a few locations, so an alternative approach was needed to address a broader geographic perspective. Our indirect approach, similar to the approaches used on a regional scale by Carey and Buffalo (2007) and by Lang and Rutledge (2011), was to analyze 11 years of cloud-to-ground (CG) data over the CONUS from the NLDN under the hypothesis that storms whose CG

Table 2
Effect Size (Lower Line) and Percent Difference in the Median Values (Upper Line) of Each Environmental Parameter in Each Region, for All 17 Parameters Analyzed in This Study

	SW	NW	SC	CC	NC	SE	NE
Cloud Base Height	-30 0.37	-23 0.23	15 0.17	20 0.23	-19 0.19	-28 0.38	-3.1 0.06
Warm Cloud Depth	29 0.36	27* 0.10*	-19 0.30	-32 0.52	16 0.18	3.2 0.16	-3.5 0.16
Dew Point Depression	-24 0.33	-8.5 0.13	9.6 0.11	30 0.31	-21 0.22	-27 0.32	3.9 0.06
Precipitable Water	3.3 0.07	-0.59* 0.02*	-17 0.48	-24 0.81	6.5 0.18	-7.6 0.36	-5.7 0.26
θ_e	0.73 0.35	0.17* 0.07*	-1.0 0.39	-1.1 0.37	1.1 0.31	-0.66 0.21	0.25 0.07
LFC to EL CAPE	60 0.47	14* 0.09*	24 0.25	-8.4 0.08	55 0.49	1.7* 0.03*	31 0.40
LFC to EL NCAPE	44 0.47	8.7* 0.08*	30 0.39	3.4 0.04	43 0.49	5.6 0.10	33 0.52
LFC to -20°C CAPE	46 0.44	17 0.13	17 0.19	-19 0.18	48 0.44	-0.50* 0.01*	25 0.35
LFC to -20°C NCAPE	36 0.44	8.4* 0.09*	26 0.39	-0.45* 0.01*	37 0.47	2.6* 0.05*	26 0.46
0°C to -20°C CAPE	39 0.45	17 0.14	29 0.39	-4.0 0.04	46 .49	5.2 0.10	34 0.51
0°C to -20°C NCAPE	39 0.46	13 0.13	30 0.41	-3.1 0.04	45 0.50	5.9 0.12	33 0.53
|CIN|	-1.3* 0.01*	-27 0.20	51 0.33	36 0.23	-12 0.07	26 0.08	27 0.14
Equilibrium Level	13 0.41	2.0* 0.09*	-2.4 0.13	-7.2 0.36	8.7 0.45	-2.9 0.19	0.11* 0.01*
0-3 km Shear	22 0.31	1.5* 0.03*	26 0.40	10 0.19	5.8 0.12	35 0.38	26 0.48
0-6 km Shear	16 0.24	-1.1* 0.02*	43 0.70	20 0.38	7.9 0.18	48 0.45	28 0.52
Storm-relative Wind Speed at EL	6.3 0.08	-6.3* 0.10*	47 0.61	15 0.22	4.4 0.06	18 0.20	17 0.22
Storm-relative Helicity	33 0.34	2.1* 0.03*	38 0.39	8.2 0.09	8.6 0.10	50 0.32	40 0.48

Note. An asterisk indicates the +CG median was not significantly different from the −CG median at the 95% level for the grid cell's parameter and region. Cell color indicates the group to which a cell belongs: green, for moisture parameters; gold, for thermodynamic parameters; and blue, for dynamic parameters. For percent difference, the darkest shading indicates the two regions with the largest values of the appropriate sign for the hypothesized enhancement of +CG production (SC and NE had a tie for second place for 0–3 km wind shear), the medium shading indicates all other regions in which the parameter's effect was consistent with the hypothesis, and the lightest shading indicates the parameter's relationship was not consistent with the hypothesis. For effect size, shading indicates broad categories of magnitude: darkest, ≥0.30; medium, ≤0.29, but consistent with hypothesized effect enhancing +CG production; lightest, medians not significantly different or inconsistent with the hypothesized effect.

Abbreviations: CAPE, convective available potential energy; CC, central-central; CIN, convective inhibition; EL, equilibrium level; θ_e, equivalent potential temperature; LFC, level of free convection; NCAPE, normalized CAPE; NC, northcentral; NE, northeast; NW, northwest; SC, southcentral; SE, southeast; SW, southwest.

activity was strongly dominated by +CG flashes have inverted-polarity charge distributions, as has been observed for storms in the CC region.

5.1. Identifying +CG-Dominated Cells and −CG-Dominated Cells

We considered three issues in our approach:

1. As detailed in Section 2.1, the 15 kA threshold for +CG peak currents, used by the NLDN during the period we analyzed (Cummins & Murphy, 2009), strikes a balance between not eliminating many valid +CG flashes and accepting contamination by some intracloud processes that the NLDN misclassifies as +CG strokes. We applied it also to −CG flashes because Fleenor et al. (2009) found that the NLDN similarly misclassified some intracloud processes as small peak current −CG strokes in inverted-polarity storms. From studies by Biagi et al. (2007) and Fleenor et al. (2009) with verification data, Murphy et al. (2020) indicated that 13% of +CG strokes identified by the NLDN with peak currents ≥ 15 kA during the period we analyzed were misidentified intracloud processes, a rate of misidentification unlikely to invalidate the trends we observed
2. As described in Section 2.1, we reduced double counting of cells by eliminating duplicates that overlapped in time or space. If two cells partially overlapped in space and occurred within 30 min of each other, only the cell with the greatest number of CG flashes was kept for analysis. Even so, some pairs of storm cells in the data set may well not be statistically independent, which would artificially inflate significance levels. However, because most of the significance levels for median differences in environmental parameters for the two cell types were very high, it is likely that many of the relationships found in this study would still exhibit a high degree of significance even if any remaining dependence between cells was completely removed
3. We chose a much higher and a much lower threshold than used previously for the fraction of CGs composed of +CGs, to make it much more likely that the storm cells we analyzed had inverted- or normal-polarity vertical charge distributions. We also limited the time of year and time of day and required a flash rate threshold that together should minimize contamination by winter storms and by the stratiform region of MCSs, because +CG domination of CG activity occurs in them for much different reasons. Previous studies (e.g., Calhoun et al., 2013; DiGangi et al., 2016; Lang et al., 2011; Rust et al., 2005) have provided a substantial data base of +CG-dominated storms in the CC region that had inverted-polarity vertical charge distributions, but this relationship is only hypothesized elsewhere. Because the NC region has a large number of suitable storms (Table 1), a field program there would likely succeed. It will be much more difficult in the remaining regions, because +CG-dominated cells are much rarer there. Although our conclusions regarding anomalous charge distributions outside the CC region are subject to verification, results concerning the environments of +CG-dominated storms themselves are still valid

This is the first CONUS-wide analysis of environmental conditions under which +CG flashes constitute a supermajority of CGs in storm cells having moderate to large CG flash rates. The geographic distribution of cells satisfying our criteria is shown in Figure 2. To analyze geographic patterns in the environmental conditions favoring +CG-dominated cells over −CG-dominated cells, we divided CONUS into seven regions (Figure 1). The result by region, shown in Table 1, is that the CC and NC regions each had more than twice as many +CG-dominated cells as any other region. Overall, the total number of cells analyzed in each region increased going from north to south and from west to east, while the fraction of analyzed cells satisfying the criteria for +CG-dominated cells increased from south to north and was largest by far in the north-central region (59%) and the central-central region (25%). These geographic trends roughly parallel what has been published in climatologies of the distribution of +CG flashes and −CG flashes in the CONUS (e.g., Boccippio et al., 2001; Orville & Huffines, 2001; Orville et al., 1987), but here the distributions are for storm cells, not individual flashes, with each analyzed cell having moderate to large CG flash rates dominated by a large fraction of either +CG or −CG flashes. Note that the north-central region was the only region in which cells satisfying our criteria for +CG-dominated cells outnumbered cells satisfying our criteria for −CG-dominated cells. Cells in which +CGs dominated CG activity constituted <4% of analyzed cells in all three southern regions and <1% in the SE.

5.2. Environmental Parameters Conducive to +CG-Dominated Cells

In choosing environmental parameters to evaluate for their impact on producing inverted polarity storms, we focused on parameters that previous studies had hypothesized would produce enhanced values of SLWC. Laboratory studies (e.g., Saunders & Peck, 1998; Takahashi, 1978) have shown that rebounding collisions between graupel and small ice particles in the presence of large SLWC causes the graupel to gain positive charge, rather than the usual negative charge, when exchanging charge with cloud ice and would cause the polarity of the storm's vertical charge distribution to be inverted from the usual polarity (with the resulting CG flashes being dominated by +CG flashes). MacGorman et al. (2008, 2011) pointed out that within updrafts in which this was true, positive charge would be the lowest charge region throughout the depth of the charging process, so the small lower negative charge thought to be needed for +CG flashes (e.g., Jacobson & Krider, 1976; Rust et al., 2005; Tessendorf, Wiens, & Rutledge, 2007) would be absent there. MacGorman et al. (2008, 2011) suggested that the lower negative charge might still be produced in adjoining regions in various ways, such as by precipitation in regions of weaker updraft or in adjoining cells that were settling as they dissipated.

Table 2 shows the effect size and percent difference in median values for each parameter in each region between storms dominated by +CG flashes and those dominated by −CG flashes. Differences hypothesized to enhance SLWC and thereby to favor +CG-dominated cells are highlighted by a darker shade of color.

To summarize and highlight results of our statistical study of the variations from region to region in the environmental effects on +CG domination, the environmental parameters that are consistent with the hypothesized effect on supercooled liquid water content in each region are ordered from the largest to smallest effect size in Table 3. (Section 2.2 describes how we computed effect size.) The results suggest that a wide variety of combinations of environmental factors can influence the production of +CG-dominated cells and, by inference, anomalous charge distributions, the lack of one or more favorable factors in a region being offset by other factors, as suggested by previous studies of the CC region.

The CC region had the largest sample of +CG-dominated cells that made it through the filtering process and is the most-studied region for environmental effects on dominant CG polarity and/or a storm's vertical distribution of charge (e.g., Carey & Buffalo, 2007; Fuchs et al., 2015; Lang & Rutledge, 2011). Although warm cloud depth and precipitable water had large effect sizes in the CC region, other moisture parameters had only small to moderate effect sizes which were smaller than the moderate effect sizes of equivalent potential temperature, equilibrium level, and 0–6 km wind shear. |CIN|, 0–3 km shear, and storm-relative wind at the EL had small effect sizes that were nearly the same as that of cloud base height.

The NC region had the second-largest number of +CG-dominated cells and was the only region to have more +CG-dominated cells than −CG-dominated cells satisfying flash rate and percentage thresholds. Yet, unlike the CC region, all of the moisture parameters favored greater SLWC in −CG-dominated cells rather than in +CG-dominated cells. On the other hand, all of the CAPE and NCAPE parameters had large percent differences and moderate to large effect sizes favoring greater SLWC in the +CG-dominated cells, and all of the dynamic parameters favored it as well, although with very small percent differences and small to very small effect sizes.

The SC region, which had the second smallest percentage of cases composed of +CG-dominated storms, was unique in that all the analyzed environmental parameters had percent differences in medians favoring hypotheses for +CG dominated cells, and it was the only region besides the CC region in which all the moisture parameters favored greater SLWC in the +CG-dominated cells. Although the moisture parameters had small to very small percent differences, the effect size was large for precipitable water and moderate for warm cloud depth. All the dynamic parameters had moderate to large effect sizes. All the thermodynamic parameters had moderate effect sizes, except LFC to EL CAPE and LFC to −20°C CAPE, which had small effect sizes, and equilibrium level, which had a very small effect size.

The SE region had the lowest percentage of cases composed of +CG-dominated storms, but all four dynamic parameters favored them, with the largest effect size being for 0–6 km wind shear. Of the moisture parameters, only precipitable water favored +CG-dominated cells, and its effect size was only moderate, comparable to that for storm-relative helicity and 0–3 km wind shear. Only three of the six parameters related to

Table 3
Environmental Parameters Favoring +CG-Dominated Cells in Each of Seven Regions Spanning the CONUS, in Descending Order of Their Effect Size

SW	NW	SC	CC	NC	SE	NE
LFC to EL CAPE 0.48	0º to -20ºC CAPE 0.14	0–6 km Wind Shear 0.70	Precipitable Water 0.81	0º to -20ºC NCAPE 0.50	0–6 km Wind Shear 0.45	0º to -20ºC NCAPE 0.53
LFC to EL NCAPE 0.47	LFC to -20ºC CAPE 0.13	Storm-relative Wind at EL 0.61	Warm Cloud Depth 0.52	LFC to EL CAPE 0.49	0–3 km Wind Shear 0.38	LFC to EL NCAPE 0.52
0º to -20ºC NCAPE 0.46	0º to -20ºC NCAPE 0.13	Precipitable Water 0.48	0–6 km Wind Shear 0.38	LFC to EL NCAPE 0.49	Precipitable Water 0.36	0–6 km Wind Shear 0.52
0º to -20ºC CAPE 0.45		0º to -20ºC NCAPE 0.41	Equivalent Potential Temperature 0.37	0º to -20ºC CAPE 0.49	Storm-relative Helicity 0.32	0º to -20ºC CAPE 0.51
LFC to -20ºC NCAPE 0.44		0–3 km Wind Shear 0.40	Equilibrium Level 0.36	LFC to -20ºC NCAPE 0.47	Equivalent Potential Temperature 0.21	Storm-relative Helicity 0.48
LFC to -20ºC CAPE 0.44		LFC to EL NCAPE 0.39	Dew Point Depression 0.31	Equilibrium Level 0.45	Storm-relative Wind at EL 0.20	0–3 km Wind Shear 0.48
Equilibrium Level 0.41		0º to -20ºC CAPE 0.39	|CIN| 0.23	LFC to -20ºC CAPE 0.44	Equilibrium Level 0.19	LFC to -20ºC NCAPE 0.46
Storm-relative Helicity 0.34		LFC to -20ºC NCAPE 0.39	Cloud Base Height 0.23	0–6 km Wind Shear 0.18	0º to -20ºC NCAPE 0.12	LFC to EL CAPE 0.40
0–3 km Wind Shear 0.31		Equivalent Potential Temperature 0.39	Storm-relative Wind at EL 0.22	0–3 km Wind Shear 0.12	0º to -20ºC CAPE 0.10	LFC to -20ºC CAPE 0.35
0–6 km Wind Shear 0.24		Storm-relative Helicity 0.39	0–3 km Wind Shear 0.19	Storm-relative Helicity 0.10	LFC to EL NCAPE 0.10	Precipitable Water 0.26
Storm-relative Wind at EL 0.08		|CIN| 0.33	Storm-relative Helicity 0.09	Storm-relative Wind at EL 0.06	|CIN| 0.08	Storm-relative Wind at EL 0.22
		Warm Cloud Depth 0.30	LFC to EL NCAPE 0.04			Warm Cloud Depth 0.16
		LFC to EL CAPE 0.25				|CIN| 0.14
		LFC to -20ºC CAPE 0.19				Dew Point Depression 0.06
		Cloud Base Height 0.17				
		Equilibrium Level 0.13				
		Dew Point Depression 0.11				

Note. Only parameters with a difference in median values significant at the 95% level and consistent with hypotheses favoring enhanced SLWC are shown. For each parameter, its statistical effect size is shown on the bottom line of the table cell, and the cell's shading indicates the range in which its effect size falls: gold, ≥45; pink, ≤44 & ≥30; aqua, ≤29 & ≥15; violet, <15.

Abbreviations: CAPE, convective available potential energy; CC, central-central; CIN, convective inhibition; EL, equilibrium level; θ_e, equivalent potential temperature; LFC, level of free convection; NCAPE, normalized CAPE; NC, northcentral; NE, northeast; NW, northwest; SC, southcentral; SE, southeast; SLWC, supercooled liquid water content; SW, southwest.

CAPE favored +CG-dominated cells, but all of them had relatively small percent differences, and three had a difference in medians that was not significant at the 95% level. |CIN| was the only thermodynamic parameter with a moderately large percent difference favoring +CG-dominated cells, and its effect size was small.

In the NE region, as in the SE region, all four dynamic parameters favored greater SLWC in +CG dominated storms. Three of the four had a large effect size. Unlike the SE region, all of the CAPE-related parameters had moderate to large effect sizes. Equivalent potential temperature and |CIN| had very small effect sizes, and the difference in medians for equilibrium level was not significant at the 95% level. Three of the four moisture parameters favored +CG-dominated cells, the largest effect size being a small one for precipitable water.

The environmental parameters favoring +CG-dominated cells in the SW region were the same as those in the NC region, with all CAPE related parameters and the equilibrium level having a larger effect size than all the dynamic parameters. Although the effect sizes for thermodynamic parameters were quite similar in the two regions, all the dynamic parameters had larger effect sizes in the SW than in the NC (particularly for storm-relative helicity and 0–3 km wind shear, which had moderate effect sizes in the SW).

Compared to all other regions, the NW region had the smallest number of cells for both dominant polarities of CGs (Table 1), consistent with it having the smallest median values of LFC to EL CAPE and of LFC to −20°C CAPE. It also had the fewest environmental parameters favoring +CG-dominated cells. The difference in medians for the moisture and dynamic parameters all either favored greater SLWC in the −CG-dominated cells or were not significantly different. The only parameters with statistically significant differences favoring +CG-dominated cells were three of the six CAPE-related parameters, and their effect sizes were all very small. The lack of parameters with larger effect sizes may mean that the nature of the cells dominated by +CGs in the NW differed markedly from the storm scenarios we intended to study. Fuquay (1982), for example, observed that CG flashes during the final 30 min of mountain storms in the NW often tended to be +CG flashes, and it is possible that +CG flash rates in such storms would occasionally meet our flash rate threshold, even though the storms were dissipating.

Previous studies of environmental parameters associated with storms having unusually large +CG fractions of CG flash activity or inverted polarity storms have all involved parts of the CC region. For example, on the basis of climatologies showing that +CG flashes comprised a larger fraction of CG flashes over the western part of the High Plains (e.g., Boccippio et al., 2001; Orville & Huffines, 2001) where storms tend to have higher cloud base heights, Williams et al. (2005) suggested that the combination of greater CAPE and elevated cloud base height in strong storms there play an important role in increasing SLWC to values sufficient to cause inverted-polarity storms, because both would reduce residence time in updrafts below the freezing level. Additionally, Williams suggested that storms with a higher CBH tend to have broader updrafts, which would reduce entrainment and mixing in the updraft core and so allow more efficient processing of CAPE and less dilution of SLWC there.

In another analysis based on regional tendencies, MacGorman et al. (2011) noted that many supercell storms in the STEPS region are LP storms and so suggested that an environmental parameter favorable to LP storms might also contribute to a greater tendency for storms in that region to have inverted-polarity charge structure. A LP storm has little precipitation in or near its strong updraft, but has most of its precipitation and hail at anvil levels. From an analysis of the environments of LP, classic, and heavy-precipitation (HP) supercell storms, Rasmussen and Straka (1998) found that LP supercell storms tend to have stronger storm-relative winds at anvil altitudes than HP storms have, while classic supercells have intermediate values. Because precipitation takes 10–30 min to form in a supersaturated parcel (e.g., Young, 1993) and the residence time of a parcel in a supercell updraft core is roughly 10 min, they suggested that precipitation in a supercell updraft probably is caused by ingesting hydrometeors from outside the updraft, as well as precipitation being grown in the fringes of the updraft. They suggested that the stronger anvil-level, storm-relative winds of LP storms tend to transport hydrometeors well away from the updraft, thereby greatly reducing the particle concentrations ingested into the updraft and accounting for the relative lack of precipitation there. MacGorman et al. (2011) noted that having fewer particles growing to precipitation size in updrafts below the mixed-phase region would mean less scavenging of cloud droplets and, therefore, a greater overall liquid water content surviving well into the mixed-phase region. Our results indicate that storm-relative wind at

the EL has a large effect size in the SC region, a small effect size in three regions including the CC region, and a very small effect size in two regions.

Two other studies of the CC region considered the effect of various environmental parameters observed by proximity soundings of many storms, somewhat similar to our approach in this study. Analyzing storms in Kansas, Oklahoma, and the Texas panhandle, Carey and Buffalo (2007) compared environmental parameters of storms in which +CGs constituted <25% of CG flashes with those of storms in which +CGs constituted >25% of CGs. In agreement with our findings, they found that storms with >25% were associated with shallower WCD, higher CBH, lower PWAT, greater DPD, greater 0–3 km shear, greater 0–3 km SRH, a lower EL, and greater LFC to EL NCAPE than storms with <25%. However, unlike our study, they found that such storms were associated with less |CIN|, and they did not find statistically significant differences for 0–6 km wind shear or for storm-relative wind speed at the EL.

Carey and Buffalo noted that precipitable water being less in storms with >25% +CGs appeared contrary to the hypothesis that greater SLWC in the mixed phase region was the primary cause of inverted polarity charge structure. They suggested that the shallower warm cloud depth, greater instability, and greater dynamical forcing that they observed would decrease particle residence time in the warm-cloud region, so as Williams (2005) suggested, more cloud droplets would survive into the mixed-phase region and increase SLWC; these parameters could more than compensate for the smaller values of adiabatic water content. They cautioned that no single environmental parameter could determine the polarity of a storm's charge distribution, but that a favorable combination could. They noted, for example, that shallow warm cloud depth and high cloud base were among the most important parameters for the mesoscale region they studied, but that high percentages of +CG flashes are seldom found in the desert southwest (where storms tend to have very high CBH), perhaps due to insufficient CAPE or to expansion of the WCD as the freezing level rose to higher altitudes during the hot afternoons of that region.

Lang and Rutledge (2011) analyzed over 28,000 storm cells from the STEPS field program and compared cells in which +CGs constituted >50% of CG flashes to those having <50%. They found that the +CG-dominated cells had an inverted-polarity structure inferred from Lightning Mapping Array data and occurred in environments having greater 0–3 km wind shear, greater 0–6 km wind shear, and greater SRH than storms having <50% +CGs, characteristics which tend to produce greater dynamical forcing of the updraft, much as we observed. However, unlike our results from the CC region, which includes the STEPS region, they found that storms with >50% +CGs were associated with environments having much greater LFC to EL CAPE, slightly lower CBHs, slightly deeper WCDs, and higher storm tops (inferred here as also meaning a higher EL). They did not consider this a refutation of the shallower WCD hypothesis for inverted-polarity storms, but instead suggested that differences in CBH and WCD may be more important when comparing storms across different regions having different environmental characteristics than when comparing storms within a given region.

Rather than analyzing CG data, Fuchs et al. (2015) studied LMA data to infer anomalous and normal storm charge distributions based on the height of positive charge inferred from mapped lightning flashes. They compared the environments of anomalous and normal polarity storms in Oklahoma and in northeastern Colorado, as well as in two other locations in which they found no storms with anomalous charge distribution. In Oklahoma, the environments of anomalously polarized storms had larger LFC to EL NCAPE than in Colorado, but Colorado had higher CBHs and larger N40 aerosol concentrations. We did not study aerosols, but their observation of higher CBHs and smaller NCAPE in Colorado agrees with our results for the CC region. Although both of the regions for which they analyzed anomalous charge distributions are within our CC region, the fraction of storms with anomalous vertical polarity tends to be larger in Colorado than in Oklahoma. Note that Lang and Rutledge (2011) analyzed essentially the same region as for the Colorado storms in Fuchs et al. (2015). At least some of the difference in results between Fuchs et al. and Lang et al. may be from their different approaches. Lang et al. examined the differences between their two categories of storms in the same region, while Fuchs et al. concentrated on the differences in environments favoring +CG-dominated storms in Colorado compared with Oklahoma. When Fuchs et al. considered storms solely in Colorado, the only differences between the two categories they found were that storms with anomalous charge distributions had larger N40 aerosol concentrations and storms with normal charge distributions had greater NCAPE.

Note that the differences in methodology, regions, and periods analyzed among these studies and between these studies and our study could all affect the differences in the environmental properties they identified as distinguishing between storms with anomalous charge distributions or larger +CG fractions and storms with normal charge distributions or smaller +CG fractions. Furthermore, one should be somewhat cautious when interpreting our results in Table 3 as being a list of the necessary ingredients in each region. It is possible, for example, that the influence of moisture parameters in the CC region may have been due in part to the geographic distributions of the two categories of storm cells: Figure 1 shows that the northern part of the CC region had much larger numbers of +CG-dominated cells than the southern portion, while the southern portion had much larger numbers of −CG-dominated cells. The northern portion tends to have higher cloud base heights and shallower warm cloud depths than the southern region, according to Fuchs et al. (2015). Thus, as suggested by the findings of Lang and Rutledge (2011) and Fuchs et al. (2015), the importance given to moisture parameters in the CC region in our study may have been due more to the climatological difference in the moisture parameters between the northern and southern parts of the region rather than due to differences that would be valid across the northern part of the CC region alone.

Similarly, the lack of a strong impact by a particular parameter does not necessarily mean that the parameter is always unimportant. It is possible that climatological differences in that parameter for all storms in a region may interact with other environmental parameters to allow differences in the other parameters to contribute to producing +CG-dominated storms, even if variations in the parameter itself provide little or no discrimination between +CG-dominated and −CG-dominated storms within the region. The NW region, for example, had median values of CBH and WCD that were even higher and lower, respectively, than in the CC region, although the medians of these parameters in the NW appeared even more conducive to greater SLWC for −CG-dominated storms. It is possible that most storms in the NW region have high enough cloud base heights and small enough warm-cloud depths to aid the relatively small differences in CAPE-related parameters that favor +CG-dominated cells, even though our hypotheses regarding the impact of CBH and WCD alone does not favor such storms when restricted to that region. Similar arguments could be made for other regions in which CBH and WCD are comparable to those in the CC region, but are more favorable for enhanced SLWC in −CG-dominated storms. What our results do suggest, however, is that particular CBH and WCD values are insufficient in themselves to contribute to +CG-dominated cells without the interaction of other parameters.

Additionally, other parameters not explored in this study, such as the aerosol concentration noted by Fuchs et al. (2015), likely influence the dominant polarity of a storm cell. Fuchs et al. (2015) found that anomalously charged thunderstorms in Colorado had greater aerosol concentrations and hypothesized that the higher concentrations of cloud condensation nuclei led to smaller drop sizes, which reduced collision-coalescence processes. Similarly, Lyons et al. (1998) and Rudlosky and Fuelberg (2011) found that +CG flash rates were greatly enhanced in storms that ingested smoke from forest fires. The link between inverted-polarity storms and greater aerosol concentrations has been inferred outside of the United States as well. Pawar et al. (2017) found that storms with inverted-polarity charge structure in India during the drier pre-monsoon season likely had greater aerosol concentrations, in addition to higher CBHs and greater DPDs. All of the inverted-polarity thunderstorms analyzed in Pawar et al. (2017) occurred on days with greater aerosol optical depth than occurred on days with normal-polarity storms. Ammonia concentration may be another factor. Marchand et al. (2019) and Chronis (2016) noted that regions of the CONUS with greater ammonia emissions coincided with local maxima in inverted-polarity IC flashes.

5.3. Summary

This was the first CONUS-wide analysis of storms cells producing moderate to large CG flash rates dominated by large percentages (≥90%) of −CG flashes or (≥80%) of +CG flashes. We infer that the +CG dominated cells had anomalous charge distributions whose dominant vertical polarity was inverted from the usual polarity, although this remains to be demonstrated directly in regions outside the CC region. Such storm cells were identified in all regions we analyzed, although most were in the central and north-central United States. In the ensemble of storms we analyzed, +CG-dominated cells constituted 25% of the storm cells in the central region and 59% in the northcentral region, but less than 4% in most other regions.

We analyzed 17 parameters in the near-storm environment of these storms in seven regions spanning CONUS, seeking to identify environmental characteristics conducive to +CG-dominated storm cells and, by inference, to inverted-polarity storms. These parameters were divided among moisture, thermodynamic, and dynamic parameters, all of which were hypothesized to be capable of contributing to anomalous charge distributions by increasing the SLWC in storm updrafts. We found, in agreement with previous studies of parts of the CC region, that no single environmental parameter or consistent set of environmental parameters characterizes the near-storm environments of +CG-dominated storms across all regions. Parameters that appeared to be strongly associated with +CG-dominated storms in some regions were not associated with +CG-dominated storms at all in other regions. It appears that a set of parameters that is favorable in one region can compensate for other parameters that are unfavorable in allowing the development and maintenance of inverted-polarity storms.

Nevertheless, if one considers the environmental parameters in Table 3 in similar groups in various regions, rather than considering the specific parameters within the groups, a dynamic parameter had a large to moderate effect size in five regions (SW, SC, CC, SE, and NE), a thermodynamic parameter had a large to moderate effect size in four regions (SW, SC, NC, and NE), and a moisture parameter had a large to moderate effect size in three regions (SC, CC, and SE). The NW region was the only one in which no parameter had a large to moderate effect size; only thermodynamic parameters favored +CG-dominated storms there, and their percent differences were small and their effect sizes were very small. Perhaps other environmental parameters or storm scenarios that we did not analyze were more relevant in the NW.

There were also some broader regional trends: In the western and northern regions, one of the forms of CAPE provided among the larger percent differences and effect sizes. In the southcentral, southeast, and northeast regions, 0–6 km wind shear had the largest effect size and so best distinguished between +CG-dominated cells and −CG-dominated cells. The SC region was the only region in which all of the parameters could favor +CG-dominated cells, although some of the effect sizes and percent differences were small to very small. The CC and the SC regions were the only ones in which all of the moisture parameters favored +CG-dominated cells. Overall, it appears that parameters favoring stronger storm updrafts in some way are important in producing +CG-dominated storms and, by inference, inverted polarity storms, as was suggested by Williams et al. (2005).

Data Availability Statement

The archived CG flash data used in this study from the National Lightning Detection Network (NLDN) belong to Vaisala. They were purchased annually by the National Weather Service and the National Severe Storms Laboratory under a federal contract that released the data to those performing basic and applied research in the purchasing organizations. These data are available for purchase or license from Vaisala by contacting B. Pearson (brook.pearson@vaisala.com) or by submitting the online request form at https://www.vaisala.com/en/lp/contact-form. North America Regional Reanalysis (NARR) data were obtained freely from UCAR at https://rda.ucar.edu/datasets/ds608.0/index.html#sfol-wl-/data/ds608.0?g=3. See Section 2 of this manuscript for a description of the NARR grid. Also see Mesinger et al. (2006) and NCAR/UCAR (2020) for more information about the NARR data set. Details, including the exact coordinates of the analysis domain and the specific vertical levels of NARR data used in this study, are available in Section 2 of Eddy (2018).

Acknowledgments
The authors thank Kristin Calhoun for providing the scripts that we modified to create the violin plots, Jason Furtado and Michael Richman for helping with the statistical analysis, and Conrad Ziegler for providing the script to perform the Lambert Conformal projection and for helpful discussions. We also thank Tracy Reinke and Jaimie Foucher of OU/CIMMS and Alan Gerard and Eric Ice of NSSL for providing administrative support for this project. Funding for this study was provided by NSF grants AGS-1063945 and AGS-1523331. Funding was also provided by NOAA/Office of Oceanic and Atmospheric Research under NOAA-University of Oklahoma Cooperative Agreement #NA11OAR4320072, U.S. Department of Commerce.

References

Alpha, T. R., & Snyder, J. P. (1982). *The properties and uses of selected map projections*. United States Geological Survey. Retrieved from https://pubs.usgs.gov/pp/1395/plate-1.pdf

An, N., Pinker, R. T., Wang, K., Rogers, E., & Zuo, Z. (2020). Evaluation of cloud base height in the North American Regional Reanalysis using ceilometer observations. *International Journal of Climatology*, *40*, 3161–3178. https://doi.org/10.1002/joc.6389

Biagi, C. J., Cummins, K. L., Kehoe, K. E., & Krider, E. P. (2007). National lightning detection network (NLDN) performance in southern Arizona, Texas, and Oklahoma in 2003–2004. *Journal of Geophysical Research*, *112*, D05208. https://doi.org/10.1029/2006JD007341

Boccippio, D. J., Cummins, K. L., Christian, H. J., & Goodman, S. J. (2001). Combined satellite- and surface-based estimation of the intracloud–cloud-to-ground lightning ratio over the continental United States. *Monthly Weather Review*, *129*, 108–122. https://doi.org/10.1175/1520-0493(2001)129<0108:csasbe>2.0.co;2

Branick, M. L., & Doswell, C. A., III (1992). An observation of the relationship between supercell structure and lightning ground-strike polarity. *Weather and Forecasting*, *7*, 143–149. https://doi.org/10.1175/1520-0434(1992)007<0143:aootrb>2.0.co;2

Bruning, E. C., Rust, W. D., MacGorman, D. R., Biggerstaff, M. I., & Schuur, T. J. (2010). Formation of charge structures in a supercell. *Monthly Weather Review*, *138*, 3740–3761, https://doi.org/10.1175/2010MWR3160.1

Bruning, E. C., Weiss, S. A., & Calhoun, K. M. (2014). Continuous variability in thunderstorm primary electrification and an evaluation of inverted-polarity terminology. *Atmospheric Research*, *135–136*, 274–284. https://doi.org/10.1016/j.atmosres.2012.10.009

Calhoun, K. M., MacGorman, D. R., Ziegler, C. L., & Biggerstaff, M. I. (2013). Evolution of lightning activity and storm charge relative to dual-Doppler analysis of a high-precipitation supercell storm. *Monthly Weather Review*, *141*(7), 2199–2223. https://doi.org/10.1175/mwr-d-12-00258.1

Carey, L. D., & Buffalo, K. M. (2007). Environmental control of cloud-to-ground lightning polarity in severe storms. *Monthly Weather Review*, *135*(4), 1327–1353. https://doi.org/10.1175/mwr3361.1. https://doi.org/10.1175/MWR3361.1

Chronis, T. (2016). *Possible effects of ammonium on lightning properties. 18th Conference of Atmospheric Chemistry. Paper 3.4*. New Orleans: American Meteorological Society. Retrieved from https://ams.confex.com/ams/96Annual/webprogram/Paper278840.html/

Cohen, J. (1988). *Statistical power analysis for the behavioral sciences*. New York: Routledge Academic. Retrieved from https://www.routledge.com/Statistical-Power-Analysis-for-the-Behavioral-Sciences/Cohen/p/book/9780805802832

Cooray, V. (2015). *An introduction to lightning*. Springer. https://doi.org/10.1007/978-94-017-8938-7

Cumming, G. (2012). *Understanding the new statistics: Effect sizes, confidence intervals, and meta-analysis*. New York: Routledge. Retrieved from https://www.routledge.com/Understanding-The-New-Statistics-Effect-Sizes-Confidence-Intervals-and/Cumming/p/book/9780415879682

Cummins, K. L., & Murphy, M. J. (2009). An overview of lightning locating systems: History, techniques, and data uses, with an in-depth look at the U.S. NLDN. *IEEE Transactions on Electromagnetic Compatibility*, *51*(3), 499–518. https://doi.org/10.1109/temc.2009.2023450

Curran, E. B., & Rust, W. D. (1992). Positive ground flashes produced by low-precipitation thunderstorms in Oklahoma on 26 April 1984. *Monthly Weather Review*, *120*, 544–553. https://doi.org/10.1175/1520-0493(1992)120<0544:pgfpbl>2.0.co;2

DiGangi, E. A., MacGorman, D. R., Ziegler, C. L., Betten, D., Biggerstaff, M., Bowlan, M., & Potvin, C. (2016). An overview of the 29 May 2012 Kingfisher supercell during DC3. *Journal of Geophysical Research: Atmospheres*, *121*, 14316–14343. https://doi.org/10.1002/2016jd025690

Eddy, A. J. (2018). *Environmental conditions producing thunderstorms with anomalous vertical polarity of charge structure (Master's Thesis)*. Norman: The University of Oklahoma. Retrieved from SHAREOK https://hdl.handle.net/11244/299935

Emersic, C., & Saunders, C. P. R. (2010). Further laboratory investigations into the relative diffusional growth rate theory of thunderstorm electrification. *Atmospheric Research*, *98*, 327–340. https://doi.org/10.1016/j.atmosres.2010.07.011

Engholm, C. D., Williams, E. R., & Dole, R. M. (1990). Meteorological and electrical conditions associated with positive cloud-to-ground lightning. *Monthly Weather Review*, *118*, 470–487. https://doi.org/10.1175/1520-0493(1990)118<0470:maecaw>2.0.co;2

Fleenor, S. A., Biagi, C. J., Cummins, K. L., Krider, E. P., & Shao, X.-M. (2009). Characteristics of cloud-to-ground lightning in warm-season thunderstorms in the Central Great Plains. *Atmospheric Research*, *91*, 333–352. https://doi.org/10.1016/j.atmosres.2008.08.011

Fuchs, B. R., Rutledge, S. A., Bruning, E. C., Pierce, J. R., Kodros, J. K., Lang, T. J., et al. (2015). Environmental controls on storm intensity and charge structure in multiple regions of the continental United States. *Journal of Geophysical Research: Atmospheres*, *120*, 6575–6596. https://doi.org/10.1002/2015jd023271

Fuchs, B. R., Rutledge, S. A., Dolan, B., Carey, L. D., & Schultz, C. (2018). Microphysical and kinematic processes associated with anomalous charge structures in isolated convection. *Journal of Geophysical Research–D: Atmospheres*, *123*, 6505–6528. https://doi.org/10.1029/2017jd027540

Fuquay, D. M. (1982). Positive cloud-to-ground lightning in summer thunderstorms. *Journal of Geophysical Research*, *87*, 7131–7140. https://doi.org/10.1029/jc087ic09p07131

Jacobson, E. A., & Krider, E. P. (1976). Electrostatic field changes produced by Florida lightning. *Journal of the Atmospheric Sciences*, *33*, 103–117. https://doi.org/10.1175/1520-0469(1976)033<0103:efcpbf>2.0.co;2

Jayaratne, E. R., Saunders, C. P. R., & Hallett, J. (1983). Laboratory studies of the charging of soft-hail during ice crystal interactions. *Quarterly Journal of the Royal Meteorological Society*, *109*(461), 609–630. https://doi.org/10.1002/qj.49710946111

Knapp, D. I. (1994). *Using cloud-to-ground lightning data to identify tornadic thunderstorm signatures and nowcast severe weather*. White Sands Missile Range: US Army Research Laboratory.

Krider, E. P., Noggle, R. C., Pifer, A. E., & Vance, D. L. (1980). Lightning direction-finding systems for forest fire detection. *Bulletin of the American Meteorological Society*, *61*, 980. https://doi.org/10.1175/1520-0477(1980)061<0980:ldfsff>2.0.co;2

Lang, T. J., Miller, L. J., Weisman, M., Rutledge, S. A., Barker, L. J., Bringi, V. N., et al. (2004). The severe thunderstorm electrification and precipitation study. *Bulletin of the American Meteorological Society*, *85*(8), 1107–1126. https://doi.org/10.1175/bams-85-8-1107

Lang, T. J., & Rutledge, S. A. (2011). A framework for the statistical analysis of large radar and lightning datasets: Results from STEPS 2000. *Monthly Weather Review*, *139*(8), 2536–2551. https://doi.org/10.1175/mwr-d-10-05000.1

Leal, A. F. R., Rakov, V. A., & Rocha, B. R. P. (2019). Compact intracloud discharges: New classification of field waveforms and identification by lightning locating systems. *Electric Power Systems Research*, *173*, 251–262. https://doi.org/10.1016/j.epsr.2019.04.016

Lyons, W. A., Nelson, T. E., Williams, E. R., Cramer, J. A., & Turner, T. R. (1998). Enhanced positive cloud-to-ground lightning in thunderstorms ingesting smoke from fires. *Science*, *282*(282), 77–80. https://doi.org/10.1126/science.282.5386.77

MacGorman, D. R., Apostolakopoulos, I. R., Lund, N. R., Demetriades, N. W. S., Murphy, M. J., & Krehbiel, P. R. (2011). The timing of cloud-to-ground lightning relative to total lightning activity. *Monthly Weather Review*, *139*(12), 3871–3886. https://doi.org/10.1175/mwr-d-11-00047.1

MacGorman, D. R., & Burgess, D. W. (1994). Positive cloud-to-ground lightning in tornadic storms and hailstorms. *Monthly Weather Review*, *122*(8), 1671–1697. https://doi.org/10.1175/1520-0493(1994)122<1671:pctgli>2.0.co;2

MacGorman, D. R., Elliott, M. S., & DiGangi, E. (2017). Electrical discharges in the overshooting tops of thunderstorms. *Journal of Geophysical Research: Atmospheres*, *122*(5), 2929–2957. https://doi.org/10.1002/2016jd025933

MacGorman, D. R., & Morgenstern, C. D. (1998). Some characteristics of cloud-to-ground lightning in mesoscale convective systems. *Journal of Geophysical Research*, *103*, 14011–14023. https://doi.org/10.1029/97jd03221

MacGorman, D. R., Rust, W. D., Krehbiel, P., Rison, W., Bruning, E., & Wiens, K. (2005). The electrical structure of two supercell storms during STEPS. *Monthly Weather Review*, *133*(9), 2583–2607. https://doi.org/10.1175/mwr2994.1

MacGorman, D. R., Rust, W. D., Schuur, T. J., Biggerstaff, M. I., Straka, J. M., Ziegler, C. L., et al. (2008). TELEX: The thunderstorm electrification and lightning experiment. *Bulletin of the American Meteorological Society*, *89*, 997–1014. https://doi.org/10.1175/2007bams2352.1

MacGorman, D. R., & Taylor, W. L. (1989). Positive cloud-to-ground lightning detection by a direction-finder network. *Journal of Geophysical Research*, *94*, 13313–13318. https://doi.org/10.1029/jd094id11p13313

Maddox, R. A., Howard, K. W., Bartels, D. L., & Rodgers, D. M. (1986). Mesoscale convective complexes in the middle latitudes. In P. S. Ray (Ed.), *Mesoscale meteorology and forecasting* (pp. 390–413). Boston: American Meteorological Society. https://doi.org/10.1007/978-1-935704-20-1_17

Makowski, J. A., MacGorman, D. R., Biggerstaff, M. I., & Beasley, W. H. (2013). Total lightning characteristics relative to radar and satellite observations of Oklahoma mesoscale convective systems. *Monthly Weather Review*, *141*(5), 1593–1611. https://doi.org/10.1175/mwr-d-11-00268.1

Marchand, M., Hilburn, K., & Miller, S. D. (2019). Geostationary lightning mapper and Earth networks lightning detection over the contiguous United States and dependence on flash characteristics. *Journal of Geophysical Research: Atmospheres*, *124*. https://doi.org/10.1029/2019jd031039

Medici, G., Cummins, K. L., Cecil, D. J., Koshak, W. J., & Rudlosky, S. D. (2017). The intracloud lightning fraction in the contiguous United States. *Monthly Weather Review*, *145*(11), 4481–4499. https://doi.org/10.1175/mwr-d-16-0426.1

Mesinger, F., DiMego, G., Kalnay, E., Mitchell, K., Shafran, P. C., Ebisuzaki, W., et al. (2006). North American regional reanalysis. *Bulletin of the American Meteorological Society*, *87*(3), 343–360. https://doi.org/10.1175/bams-87-3-343

Murphy, M. J., Cramer, J. A, & Said, R. K. (2020). Recent history of upgrades to the U. S. National Lightning Detection Network. *Journal of Atmospheric and Oceanic Technology*, *38*(3), 573–585. https://doi.org/10.1175/JTECH-D-19-0215.1

Nag, A., Murphy, M. J., & Cramer, J. A. (2016). Update to the U.S. National Lightning Detection Network. *Paper presented at 24th International Lightning Detection Conference (ILDC), San Diego*.

NCAR/UCAR. (2020). *Research data archive: Computational & information systems lab*. Retrieved from rda.ucar.edu

Orville, R. E. (2008). Development of the National Lightning Detection Network. *Bulletin of the American Meteorolical Society*, *89*, 180–190. https://doi.org/10.1175/bams-89-2-180

Orville, R. E., & Huffines, G. R. (2001). Cloud-to-ground lightning in the United States: NLDN results in the first decade, 1989–98. *Monthly Weather Review*, *129*, 1179–1193. https://doi.org/10.1175/1520-0493(2001)129<1179:ctglit>2.0.co;2

Orville, R. E., Weisman, R. A., Pyle, R. B., Henderson, R. W., & Orville, R. E., Jr. (1987). Cloud-to-ground lightning flash characteristics from June 1984 through May 1985. *Journal of Geophysical Research*, *92*, 5640–5644. https://doi.org/10.1029/jd092id05p05640

Pawar, S. D., Gopalakrishnan, V., Murugavel, P., Veremey, N. E., & Sinkevich, A. A. (2017). Possible role of aerosols in the charge structure of isolated thunderstorms. *Atmospheric Research*, *183*, 331–340. https://doi.org/10.1016/j.atmosres.2016.09.016

Rasmussen, E. N., & Straka, J. M. (1998). Variations in supercell morphology. Part I: Observations of the role of upper-level storm-relative flow. *Monthly Weather Review*, *126*, 2406–2421. https://doi.org/10.1175/1520-0493(1998)126<2406:vismpi>2.0.co;2

Rasmussen, K. L., & Houze, R. A., Jr. (2016). Convective initiation near the Andes in subtropical South America. *Monthly Weather Review*, *144*(6), 2351–2374. https://doi.org/10.1175/mwr-d-15-0058.1

Reap, R. M., & MacGorman, D. R. (1989). Cloud-to-ground lightning: Climatological characteristics and relationships to model fields, radar observations, and severe local storms. *Monthly Weather Review*, *117*, 518–535. https://doi.org/10.1175/1520-0493(1989)117<0518:ctglcc>2.0.co;2

Rudlosky, S. D., & Fuelberg, H. E. (2011). Seasonal, regional, and storm-scale variability of cloud-to-ground lightning characteristics in Florida. *Monthly Weather Review*, *139*(6), 1826–1843. https://doi.org/10.1175/2010mwr3585.1

Rust, W. D., & MacGorman, D. R. (2002). Possibly inverted-polarity electrical structures in thunderstorms during STEPS. *Geophysical Research Letters*, *29*(12). https://doi.org/10.1029/2001gl014303

Rust, W. D., MacGorman, D. R., Bruning, E. C., Weiss, S. A., Krehbiel, P. R., Thomas, R. J., et al. (2005). Inverted-polarity electrical structures in thunderstorms in the Severe Thunderstorm Electrification and Precipitation Study (STEPS). *Atmospheric Research*, *76*, 247–271. https://doi.org/10.1016/j.atmosres.2004.11.029

Rutledge, S. A., & MacGorman, D. R. (1988). Cloud-to-ground lightning activity in the 10–11 June 1985 mesoscale convective system observed during the Oklahoma-Kansas PRE-STORM project. *Monthly Weather Review*, *116*(7), 1393–1408. https://doi.org/10.1175/1520-0493(1988)116<1393:ctglai>2.0.co;2

Rutledge, S. A., Williams, E. R., & Petersen, W. A. (1993). Lightning and electrical structure of mesoscale convective systems. *Atmospheric Research*, *29*, 27–53. https://doi.org/10.1016/0169-8095(93)90036-n

Saunders, C. P. R., & Peck, S. L. (1998). Laboratory studies of the influence of the rime accretion rate on charge transfer during crystal/graupel collisions. *Journal of Geophysical Research*, *103*(D12), 13949–13956. https://doi.org/10.1029/97jd02644

Seimon, A. (1993). Anomalous cloud-to-ground lightning in an F5-tornado-producing supercell thunderstorm on 28 August 1990. *Bulletin of the American Meteorological Society*, *74*, 189–203. https://doi.org/10.1175/1520-0477(1993)074<0189:actgli>2.0.co;2

Shao, X.-M., Stanley, M., Regan, A., Harlin, J., Pongratz, M., & Stock, M. (2006). Total lightning observations with the new and improved Los Alamos Sferic Array (LASA). *Journal of Atmospheric and Oceanic Technology*, *23*, 1273–1288. https://doi.org/10.1175/jtech1908.1

Smith, S. B., LaDue, J. G., & MacGorman, D. R. (2000). The relationship between cloud-to-ground lightning polarity and surface equivalent potential temperature during three tornadic outbreaks. *Monthly Weather Review*, *128*, 3320–3328. https://doi.org/10.1175/1520-0493(2000)128<3320:trbctg>2.0.co;2

Snyder, J. P. (1987). *Map projections: A working manual*. Washington: U.S. Government Printing Office. U.S. Geological Survey Professional Paper 1395. https://doi.org/10.2307/1774978

Takagi, N., Takeuti, T., & Nakai, T. (1986). On the occurrence of positive ground flashes. *Journal of Geophysical Research*, *91*(D9), 9905–9909. https://doi.org/10.1029/jd091id09p09905

Takahashi, T. (1978). Riming electrification as a charge generation mechanism in thunderstorms. *Journal of the Atmospheric Sciences*, *35*(8), 1536–1548. https://doi.org/10.1175/1520-0469(1978)035<1536:reaacg>2.0.co;2

Takahashi, T., & Miyawaki, K. (2002). Reexamination of riming electrification in a wind tunnel. *Journal of the Atmospheric Sciences*, *59*, 1018–1025. https://doi.org/10.1175/1520-046910.1175/1520-0469(2002)059<1018:roreia>2.0.co;2

Takeuti, T., Nakano, M., Brook, M., Raymond, D. J., & Krehbiel, P. (1978). The anomalous winter thunderstorms of the Hokuriku coast. *Journal of Geophysical Research*, *83*(C5), 2385–2394. https://doi.org/10.1029/jc083ic05p02385

Tessendorf, S. A., Rutledge, S. A., & Wiens, K. C. (2007a). Radar and lightning observations of normal and inverted polarity multicellular storms from STEPS. *Monthly Weather Review*, *135*(11), 3682–3706. https://doi.org/10.1175/2007mwr1954.1

Tessendorf, S. A., Wiens, K. C., & Rutledge, S. A. (2007b). Radar and lightning observations of the 3 June 2000 electrically inverted storm from STEPS. *Monthly Weather Review*, *135*, 3665–3681. https://doi.org/10.1175/2006mwr1953.1

Weisman, M. L., & Klemp, J. B. (1982). The dependence of numerically simulated convective storms on vertical wind shear and buoyancy. *Monthly Weather Review*, *110*, 504–520. https://doi.org/10.1175/1520-0493(1982)110<0504:tdonsc>2.0.co;2

Weisman, M. L., & Klemp, J. B. (1984). The structure and classification of numerically simulated convective storms in directionally varying wind shears. *Monthly Weather Review*, *112*, 2479–2498. https://doi.org/10.1175/1520-0493(1984)112<2479:tsacon>2.0.co;2

Weiss, S. A., Rust, W. D., MacGorman, D. R., Bruning, E. C., & Krehbiel, P. R. (2008). Evolving complex electrical structures of the STEPS 25 June 2000 multicell storm. *Monthly Weather Review*, *136*(2), 741–756. https://doi.org/10.1175/2007mwr2023.1

Wiens, K. C., Rutledge, S. A., & Tessendorf, S. A. (2005). The 29 June 2000 supercell observed during STEPS. Part II: Lightning and charge structure. *Journal of the Atmospheric Sciences*, *62*(12), 4151–4177. https://doi.org/10.1175/jas3615.1

Wilks, D. . (2011). Statistical Methods in the Atmospheric Sciences. International Geophysics (3rd ed., Vol. 100). Academic Press. https://doi.org/10.1016/B978-0-12-385022-5.00026-9

Williams, E. R., Lyons, W. A., Hobara, Y., Mushtak, V. C., Asencio, N., Boldi, R., et al. (2010). Ground-based detection of sprites and their parent lightning flashes over Africa during the 2006 AMMA campaign. *Quarterly Journal of the Royal Meteorological Society*, *136*, 257–271. https://doi.org/10.1002/qj.489

Williams, E. R., Mushtak, V., Rosenfeld, D., Goodman, S., & Boccippio, D. (2005). Thermodynamic conditions favorable to superlative thunderstorm updraft, mixed phase microphysics and lightning flash rate. *Atmospheric Research*, *76*(2005), 288–306. https://doi.org/10.1016/j.atmosres.2004.11.009

Young, K. C. (1993). *Microphysical processes in clouds*. Oxford University Press.